Annals of Botany **125**: 905–923, 2020
doi: 10.1093/aob/mcaa022, available online at www.academic.oup.com/aob

ANNALS OF BOTANY
Founded 1887

Mutational analysis indicates that abnormalities in rhizobial infection and subsequent plant cell and bacteroid differentiation in pea (*Pisum sativum*) nodules coincide with abnormal cytokinin responses and localization

Elena A. Dolgikh[1,*,†], Pyotr G. Kusakin[1,†], Anna B. Kitaeva[1], Anna V. Tsyganova[1], Anna N. Kirienko[1], Irina V. Leppyanen[1], Aleksandra V. Dolgikh[1,2], Elena L. Ilina[3], Kirill N. Demchenko[1,3], Igor A. Tikhonovich[1,2] and Viktor E. Tsyganov[1,4]

[1]All-Russia Research Institute for Agricultural Microbiology, Laboratory of Molecular and Cellular Biology, Podbelsky chaussee 3, 196608, Pushkin 8, Saint Petersburg, Russia, [2]Saint Petersburg State University, Department of Genetics and Biotechnology, Universitetskaya embankment 7–9, Saint Petersburg, 199034, Russia, [3]Komarov Botanical Institute, Russian Academy of Sciences, Laboratory of Cellular and Molecular Mechanisms of Plant Development, Prof. Popov street 2, 197376, Saint Petersburg, Russia and [4]Saint Petersburg Scientific Center Russian Academy of Sciences, Universitetskaya embankment 5, 199034, Saint Petersburg, Russia
**For correspondence. E-mail dol2helen@yahoo.com*
[†]These authors contributed equally to this work.

Received: 6 October 2019 Returned for revision: 13 December 2019 Editorial decision: 31 January 2020 Accepted: 26 February 2020
Published electronically 21 March 2020

• **Background and Aims:** Recent findings indicate that Nod factor signalling is tightly interconnected with phytohormonal regulation that affects the development of nodules. Since the mechanisms of this interaction are still far from understood, here the distribution of cytokinin and auxin in pea (*Pisum sativum*) nodules was investigated. In addition, the effect of certain mutations blocking rhizobial infection and subsequent plant cell and bacteroid differentiation on cytokinin distribution in nodules was analysed.
• **Methods:** Patterns of cytokinin and auxin in pea nodules were profiled using both responsive genetic constructs and antibodies.
• **Key Results:** In wild-type nodules, cytokinins were found in the meristem, infection zone and apical part of the nitrogen fixation zone, whereas auxin localization was restricted to the meristem and peripheral tissues. We found significantly altered cytokinin distribution in *sym33* and *sym40* pea mutants defective in IPD3/CYCLOPS and EFD transcription factors, respectively. In the *sym33* mutants impaired in bacterial accommodation and subsequent nodule differentiation, cytokinin localization was mostly limited to the meristem. In addition, we found significantly decreased expression of *LOG1* and A-type *RR11* as well as *KNOX3* and *NIN* genes in the *sym33* mutants, which correlated with low cellular cytokinin levels. In the *sym40* mutant, cytokinins were detected in the nodule infection zone but, in contrast to the wild type, they were absent in infection droplets.
• **Conclusions:** In conclusion, our findings suggest that enhanced cytokinin accumulation during the late stages of symbiosis development may be associated with bacterial penetration into the plant cells and subsequent plant cell and bacteroid differentiation.

Key words: Bacterial penetration, bacteroid differentiation, cytokinins, auxin, KNOX3 transcription factor, NIN transcription factor, immunolocalization, composite plants, pea mutants, plant cell differentiation.

INTRODUCTION

Legumes develop a structurally and functionally unique organ, the nodule, in response to inoculation with nitrogen-fixing bacteria collectively called rhizobia. *De novo* morphogenesis of nodules is induced by rhizobial signalling molecules, the Nod factors (Denarie *et al.*, 1996), as well as microRNA (miRNA) (Simon *et al.*, 2009), tRNA-derived small RNA fragments (tRFs) (Ren *et al.*, 2019) and small rDNA-derived RNA (srRNA) (Jin *et al.*, 2020); although similar to other processes associated with the development of new tissues and organs, nodule formation is also controlled by endogenous plant regulators. Multiple findings indicate that Nod factor signalling is tightly interconnected with changes in phytohormone synthesis, accumulation and perception that affect the infection and development of nodules.

Cytokinin and auxin are essential for regulating both rhizobial infection and nodule organogenesis (Thimann, 1936; Libbenga and Harkes, 1973; Cooper and Long, 1994; Mathesius *et al.*, 1998; Rightmyer and Long, 2011; Demina *et al.*, 2019). According to previous reports, the formation of auxin response maxima in various legumes precedes the initiation of nodule formation, and, most probably, results from a reduction in polar auxin transport or, alternatively, an auxin biosynthesis stimulation (Mathesius *et al.*, 1998; Boot *et al.*, 1999; Pacios-Bras *et al.*, 2003; Huo *et al.*, 2006; Suzaki *et al.*, 2012; Ng *et al.*, 2015; Schiessl *et al.*, 2019). During early nodulation stages,

some *LAX* (*LIKE-AUX1*) genes encoding auxin importers were found to be highly expressed in the developing primordia in *Medicago truncatula* (de Billy *et al.*, 2001; Roy *et al.*, 2017), suggesting that auxin plays an important role in initiating and maintaining cell proliferation to form the nodule primordia (Mathesius *et al.*, 1998; Suzaki *et al.*, 2012). In addition, auxin is involved in the regulation of infection thread progression (Breakspear *et al.*, 2014; Laplaze *et al.*, 2015).

The key role of cytokinins in nodule initiation was demonstrated by the phenotype of *M. truncatula* and *Lotus japonicus* mutants *cre1* (*cytokinin response1*) and *hit1* (*hyperinfected1*) affecting the cytokinin receptors *Mt*CRE1 and *Lj*LHK1 (Gonzalez-Rizzo *et al.*, 2006; Murray *et al.*, 2007; Plet *et al.*, 2011). The loss-of-function mutants *cre1* and *hit1* are defective in nodule formation (Gonzalez-Rizzo *et al.*, 2006; Murray *et al.*, 2007). In contrast, in the *snf2* (*spontaneous nodule formation2*) mutant carrying a gain-of-function mutation in *LjLHK1*, the development of nodule-like structures was observed in the absence of rhizobia (Tirichine *et al.*, 2007). Similarly, in *M. truncatula* plants expressing *Mt*CRE1 with an amino acid replacement in the CHASE domain (L267F), spontaneous nodules appeared (Ovchinnikova *et al.*, 2011). It has been shown that the cytokinin pathway may regulate certain flavonoids acting on polar auxin transport through its effect on PIN-formed (PIN) auxin efflux carriers, that influences auxin accumulation in cortical cells during the early stages of nodulation (Plet *et al.*, 2011; Ng *et al.*, 2015). Moreover in *L. japonicus* and *M. truncatula*, cytokinin signalling also positively regulates auxin accumulation, probably by regulating genes involved in auxin biosynthesis (Suzaki *et al.*, 2012; Schiessl *et al.*, 2019).

In accordance with the suggested involvement of cytokinins in the regulation of early stages of nodulation, the cytokinin biosynthesis genes *ISOPENTENYL TRANSFERASE* (*IPT*) and *LONELY GUY* (*LOG*) are up-regulated during these stages. *LjIPT2* and *LjIPT4* in *L. japonicus* and their homologues *MtIPT2* (Medtr4g117330) and *MtIPT4* (Medtr2g022140) in *M. truncatula* as well as *PsIPT1* and *PsIPT2* in *Pisum sativum* are quickly induced in response to rhizobial inoculation or Nod factor treatment followed by cytokinin accumulation in roots (van Zeijl *et al.*, 2015; Jardinaud *et al.*, 2016; Dolgikh *et al.*, 2017; Reid *et al.*, 2017). However, in addition to their early activation, other genes are strongly up-regulated during the late stages of nodulation, such as *LjIPT1* and *LjIPT3* in *L. japonicus*, or *MtIPT1* (Medtr1g110590) and *MtIPT3* (Medtr1g072540) in *M. truncatula* and their homologues *PsIPT4* and *PsIPT3* in *P. sativum*, respectively, as well as *MtLOG1*, *MtLOG2*, *PsLOG1* and *PsLOG2* (Chen *et al.*, 2014; Mortier *et al.*, 2014; Azarakhsh *et al.*, 2015; Dolgikh *et al.*, 2017; Reid *et al.*, 2017). Moreover, knock down of *LjIPT3* or *MtLOG1* and *MtLOG2* by RNA interference leads to decreased nodulation (Chen *et al.*, 2014; Mortier *et al.*, 2014). This suggests that cytokinin signalling activated in plant cells during the late stages of symbiosis development fulfils specific functions that remain to be elucidated. In contrast, the cytokinins produced by rhizobia are capable of influencing the efficiency of symbiosis but do not affect the formation of nodules (Kisiala *et al.*, 2013).

Genes involved in cytokinin signalling such as those encoding the B- and A-type response regulators (B- and A-type RRs) were shown to be activated in the rhizodermis and cortical cells during nodule initiation (Gonzalez-Rizzo *et al.*, 2006; Lohar *et al.*, 2006; Vernié *et al.*, 2008; Ariel *et al.*, 2012; Held *et al.*, 2014; van Zeijl *et al.*, 2015; Liu *et al.*, 2018). Recent data showed that cytokinins tightly interplay with several transcriptional regulators of nodulation such as NSP2, NIN and EFD (Vernié *et al.*, 2008; Ariel *et al.*, 2012; Liu *et al.*, 2018). It has been found that the transcription factor for cytokinin signalling, the B-type RR, activates NSP2, a key regulator of nodulation (Ariel *et al.*, 2012). Analysis of mutants showed that the response to exogenously applied cytokinins depended on NSP2 and NIN, affecting nodule development (Heckmann *et al.*, 2011). Several putative cytokinin response elements have been found in the *NIN* promoter region and shown to be important to regulate *NIN* expression in the pericycle during formation of nodule primordia (Liu *et al.*, 2018). Another transcription factor, EFD, directly regulates the A-type RR, restricting the action of cytokinin (Vernié *et al.*, 2008). Since EFD plays a positive role in nodule differentiation, the cytokinins may be involved in the regulation of the late stages of nodulation associated with rhizobial infection and subsequent plant cell and bacteroid differentiation. This suggests cross-talk between the regulators of cytokinin- and Nod factor-activated signalling, which requires further investigation.

To elucidate the specific functions of cytokinin and auxin signalling during the late stages of symbiosis development, we analysed the cytokinin and auxin dynamics in wild-type pea plants and Fix$^-$ mutants defective in the genes encoding key transcription factors IPD3/CYCLOPS (*sym33* mutants) and EFD (*sym40* mutant). The mutants in the *sym33* gene were impaired in the infection process due to the absence of bacterial release from the infection threads (Tsyganov *et al.*, 1998; Voroshilova *et al.*, 2009; Tsyganova *et al.*, 2019). The *sym40* mutant had nodules with abnormal histological organization, hypertrophied infection droplets and abnormal bacteroids (Tsyganov *et al.*, 1998). The results revealed that the cytokinin distribution was significantly altered in these mutants impaired in the late stages of nodule development. To further elucidate the link between the cytokinin response and localization and abnormalities in the late stages of nodulation, we also assessed the cytokinin distribution in pea *sym31* and *sym26* mutants defective in plant and bacteroid differentiation (Borisov *et al.*, 1997; Serova *et al.*, 2018).

MATERIALS AND METHODS

Plant material, bacterial strains and plant growth conditions

Pea (*Pisum sativum* L.) SGE and Sprint-2 wild-type lines and derived mutant lines having nodule development arrest at different stages were used in this study (Table 1). To perform gene expression studies, surface-sterilized seeds were transferred to Petri dishes with 1 % water agar and germinated in the dark at 23 °C for a 4–5 d period. Following germination, plants were transferred into pots with vermiculite and grown in a growth chamber at 21 °C and 60 % humidity in a 16 h/8 h light/dark cycle. For immunolocalization analysis, three independent experiments were performed. Surface-sterilized seeds were transferred into vermiculite supplemented with nutrient solution without nitrogen (Fåhraeus, 1957). In all experiments, the seedlings were inoculated with *Rhizobium leguminosarum* bv. *viciae* strain 3841 (Wang *et al.*, 1982). Growth conditions for plants and bacteria were as described previously (Ivanova *et al.*, 2015). Nodules were harvested 2 and 4 weeks after inoculation.

Table 1. *Plant material used in the study*

Lines	Phenotype	References
SGE	Wild type	Kosterin and Rozov (1993); Tsyganov *et al.* (1998)
SGEFix⁻-2 (*sym33-3*)	'Locked' infection threads inside the nodule, occasional bacterial release	Tsyganov *et al.* (1994, 1998, 2011); Voroshilova *et al.* (2001, 2009)
SGEFix⁻-5 (*sym33-2*)	'Locked' infection threads inside the nodule, no bacterial release	Ovchinnikova *et al.* (2011); Tsyganov *et al.* (2013); Tsyganova *et al.* (2019)
SGEFix⁻-1 (*sym40*)	Hypertrophied infection droplets and infection threads, abnormal bacteroids	Tsyganov *et al.* (1994, 1998); Voroshilova *et al.* (2009)
SGEFix⁻-3 (*sym26*)	Premature degradation of symbiotic structures	Tsyganov *et al.* (2000); Serova *et al.* (2018)
Sprint-2	Wild type	Borisov *et al.*, (1994, 1997)
Sprint-2Fix⁻ (*sym31*)	Undifferentiated bacteroids, several bacteroids are surrounded by a common symbiosome membrane	Borisov *et al.* (1994, 1997)

For each variant, 10–15 nodules from different plants were analysed.

RNA isolation and cDNA synthesis

Pea nodules were harvested 2 and 3 weeks after inoculation and frozen in liquid nitrogen. Total RNA was isolated from approx. 50–100 mg of tissue per sample using the TriZol reagent (Thermo Fisher Scientific, USA) as previously described (Azarakhsh *et al.*, 2015). RNA (1–2.5 µg) was used as template for cDNA synthesis with RevertAid Reverse Transcriptase (Thermo Fisher Scientific) for 1 h at 42 °C followed by 5 min at 95 °C. Aliquots of cDNA were diluted 1:10 for subsequent quantitative PCR analysis.

Quantitative reverse transcription–PCR (qRT–PCR) analysis

The qRT–PCR analysis was performed on a CFX-96 real-time PCR detection system with a C1000 thermal cycler (Bio-Rad Laboratories, USA). Relative expression was normalized against constitutively expressed *Ubiquitin* and *Actin* genes from pea. Each PCR was carried out with SYBR Green intercalating dye in a total volume of 10 µL. Reactions were conducted in triplicate and then averaged. Cycle threshold (Ct) values were obtained using the accompanying software, with data analysed according to the $2^{-\Delta\Delta C}{}_{T}$ method (Livak and Schmittgen, 2001). PCR primers were designed using the Vector NTI program (Thermo Fisher Scientific), with all primer sequences employed in expression analysis listed in Supplementary data Table S1. Each experiment was repeated a minimum of three times using independent biological samples (n = 3–4).

Agrobacterium rhizogenes-*mediated plant transformation*

For plant transformation, 4- to 5-day-old pea seedlings were transferred in sterile dark plastic boxes with Jensen's medium to light conditions and incubated for 3–4 d. Seedlings were cut at the hypocotyl region and transformed with freshly grown *Agrobacterium rhizogenes* strain ARqua 1 (Quandt *et al.*, 1993) carrying an appropriate plasmid. *DR5::GFP*-NLS (NLS = nuclear localization signal; Ilina *et al.*, 2018) and *MtRR4::GUS* (Plet *et al.*, 2011) were used for transformation. Plants were placed in plastic vessels (Duchefa, The Netherlands) on Jensen's agar, with the area exposed by the cut covered with wet cotton wool and aluminium foil (Leppyanen *et al.*, 2019). The seedlings were co-cultivated with *A. rhizogenes* for a period of 10–14 d at 21 °C (16 h/8 h light/darkness), transferred to Emergence medium containing 150 mg mL^{-1} cefotaxime and incubated for 3–4 d. Before transferring into pots with vermiculite saturated with Jensen's medium containing 1.5 mM NH_4NO_3, emerging roots were analysed under the fluorescent stereomicroscope on a SteREO Discovery, V8 (Zeiss, Germany). Transgenic roots were selected by visualization of *DsRED* or *GFP* (green fluorescent protein) expression. The primordia and nodules which appeared were used for GFP and β-glucuronidase (GUS) localization. To localize GFP, the roots with primordia and nodules were fixed in freshly prepared fixative solution and sectioned as previously described (Ilina *et al.*, 2018). For GUS staining, the material was fixed in freshly prepared 3 % paraformaldehyde, 0.1 % Tween-20 in phosphate-buffered saline (PBS; pH 7.4) under vacuum (–0.9 bar; ME 1C vacuum pump, Vacuubrand, Germany) for 3 min, three times at 10 min intervals. GUS staining was performed overnight at 37 °C. Imaging and analysis of sections of *DR5::GFP*-NLS-transformed nodules were carried out using the laser scanning confocal system LSM 510 META equipped with ZEN 2009 software (Zeiss). Sections of GUS-stained nodules were examined on an Axio Imager.Z1 (Zeiss) microscope, and were imaged with an Axiocam 506 colour (Zeiss) digital microscope camera. Two independent experiments were performed for each variant. A total of 10–15 nodules from different transgenic roots (n = 8–10) were used for analysis in each variant.

Trans-*zeatin riboside immunolocalization and confocal laser scanning microscopy*

For immunolocalization of *trans*-zeatin riboside, collected nodules were fixed and sectioned as described by Kitaeva *et al.* (2016) with minor changes. Material was fixed in freshly prepared fixative solution (3 % paraformaldehyde, 0.5 % glutaraldehyde, 0.1 % Tween-20, 0.1 % Triton X-100) in 1/3 MTSB (50 mM PIPES, 5 mM $MgSO_4 \cdot 7H_2O$, 5 mM

EGTA, pH 6.9) under a vacuum (−0.9 bar; ME 1C vacuum pump, Vacuubrand) for 7 min, three times at 15 min intervals. Then samples were incubated in the fixative solution overnight at 4 °C, followed by rinsing in 1/3 MTSB three times. Nodules were mounted into 3 % agarose blocks and longitudinally sectioned (50 µm) using a HM650V microtome with a vibrating blade (Microm, Germany). Sections were incubated in blocking solutions, first in 5 % bovine serum albumin (BSA), 0.5 % goat serum and 0.2 % cold fish gelatin in MTSB for 30 min at 28 °C, followed by 2 mg mL^{-1} acetylated BSA (BSA-C) in Tris-buffered saline (TBS; 50 mM Tris–HCl, 150 mM NaCl, pH 7.5) for 30 min at 28 °C. Next, sections were incubated overnight at 4 °C in 1 % BSA in TBS with primary rabbit anti-*trans*-zeatin riboside IgG or rabbit anti-N^6-isopentenyladenosine IgG (Agrisera, Sweden) at 1:100 dilution. Sections were washed in TBS ten times for 10 min then incubated in 5 % BSA in TBS for 25 min at 28 °C. Sections were then incubated in 1 % BSA in TBS with secondary goat anti-rabbit IgG Alexa Fluor 488 (Thermo Fisher Scientific) at 1:750 dilution for 90 min at 28 °C. In order to visualize nuclei and bacteria, sections were then washed three times for 10 min in TBS and stained with propidium iodide (0.5 µg mL^{-1}) for 8 min. Sections were then washed twice in TBS for 10 min and mounted under coverslips in ProLong Gold antifade reagent (Thermo Fisher Scientific).

As a positive control for the primary antibody specificity, nodules were incubated in 40 mM *trans*-zeatin riboside (Sigma-Aldrich, USA), 0.1 % Tween-20 and 0.1 % Triton X-100 in 1/3 MTSB under vacuum (−0.9 bar, three times for 20 min, at 15 min intervals) before fixation (Supplementary data Fig. S1A–C). As a blank control, nodules were fixed in FAA (3.8 % paraformaldehyde and 3.8 % acetic acid in 70 % ethanol) solution (Supplementary data Fig. S1D–F). To ensure binding specificity of secondary antibodies with primary antibodies, a negative control was performed with anti-*trans*-zeatin riboside antibody omitted during the immunolocalization protocol (Supplementary data Fig. S1G–I). Analysis of sections was carried out using the laser scanning confocal systems LSM 510 META or LSM 780 (Zeiss), equipped with ZEN 2009 or ZEN 2.3pro software (Zeiss), respectively.

Immunogold labelling and transmission electron microscopy

The immunogold labelling procedure was described previously (Tsyganova *et al.*, 2009). Sections were treated with the primary rabbit anti-*trans*-zeatin riboside IgG antibody (Agrisera) diluted 1:25 in 0.1 % BSA-C in PBS (2.48 g L^{-1} NaH_2PO_4, 21.36 g L^{-1} Na_2HPO_4, 87.66 g L^{-1} NaCl, pH 7.2) at 4 °C overnight. After rinsing four times in 0.1 % BSA-C in PBS, samples were incubated with a 10 nm gold-conjugated secondary antibody goat anti-rat IgG (Amersham International, UK), diluted 1:50 in 0.1 % BSA-C in PBS for 4 h at 37 °C. The grids containing the sections were counterstained with 2 % aqueous uranyl acetate for 1 h followed by Reynolds' lead citrate for 1 min. Nodule tissues were examined under a transmission electron microscope, JEM-1400 (Jeol, Japan), at 80 kV. Images were obtained using a Veleta side-mounted CCD camera (Olympus, Germany).

RESULTS

Cytokinin and auxin response patterns in wild-type pea nodules

The pattern of cytokinin and auxin distribution was previously investigated in wild-type nodules of model legumes *M. truncatula* and *L. japonicus*, and more recently in soybean (*Glycine max*) (Plet *et al.*, 2011; Suzaki *et al.*, 2012; Held *et al.*, 2014; Fisher *et al.*, 2018). However, there was only limited information about cytokinin and auxin localization in pea nodules. To study the importance of auxin and cytokinin in the development of nodules in pea, composite plants carrying genetic constructs with auxin- and cytokinin-responsive promoters and reporter genes *DR5::GFP*-NLS (Ilina *et al.*, 2018) and *pMtRR4::GUS* having four 12 bp RR-binding sites (RRBSs) (Ariel *et al.*, 2012) were examined. In pea SGE wild-type plants containing the *DR5::GFP*-NLS construct, the auxin response maxima were observed during the early stages of nodule development in dividing cells of the pericycle, endoderm and inner cortex of the root (Fig. 1A, B). In 2-week-old nodules, the response to auxin was localized in the meristem, bordering cells around vascular bundles and peripheral tissues (Fig. 1C; Supplementary data Fig. S2A, B). A similar pattern was found in 3-week-old nodules (Fig. 1D–F; Supplementary data Fig. S2C, D), indicating the possible role of auxin in maintaining the meristem activity and the processes occurring in the vasculature.

Analysis of transgenic roots containing the *pMtRR4::GUS* construct revealed the response to cytokinins in the primordia and emerging nodules (Fig. 2A, B). In the 2-week-old pea nodules, the GUS reporter was detected in the meristem, the infection zone and the apical part of the nitrogen fixation zone (Fig. 2C, D). These observations suggested that the cytokinins participate not only in maintaining the meristem activity in nodules, but also in controlling the late stages of the nodule development associated with the infection process and the differentiation of nodule tissue. Since our analysis indicated that cytokinins could be important for regulation of the late stages of symbiosis development, we performed a more detailed analysis of the cytokinin distribution in pea mutants defective in bacterial penetration into plant cells and subsequent tissue differentiation.

Cytokinin response patterns in sym33-2 *and* sym33-3 *mutants defective in the gene encoding the IPD3/CYCLOPS transcription factor*

The transcription factor IPD3/CYCLOPS encoded by the *Sym33* gene in pea may be involved in infection development and intracellular bacterial accommodation (Tsyganov *et al.*, 1998; Ovchinnikova *et al.*, 2011; Tsyganova *et al.*, 2019), as was shown in model legumes (Messinese *et al.*, 2007; Yano *et al.*, 2008). In addition, IPD3/CYCLOPS is also required for transactivation of NIN transcription factor, which may be important for regulation of organogenesis (Singh *et al.*, 2014). Moreover, recent studies in pea forming the indeterminate nodule type allowed the discovery of a strong mutant allele, *sym33-4*, that failed to develop nodules (Zhernakov *et al.*, 2019). The pattern of cytokinin distribution in

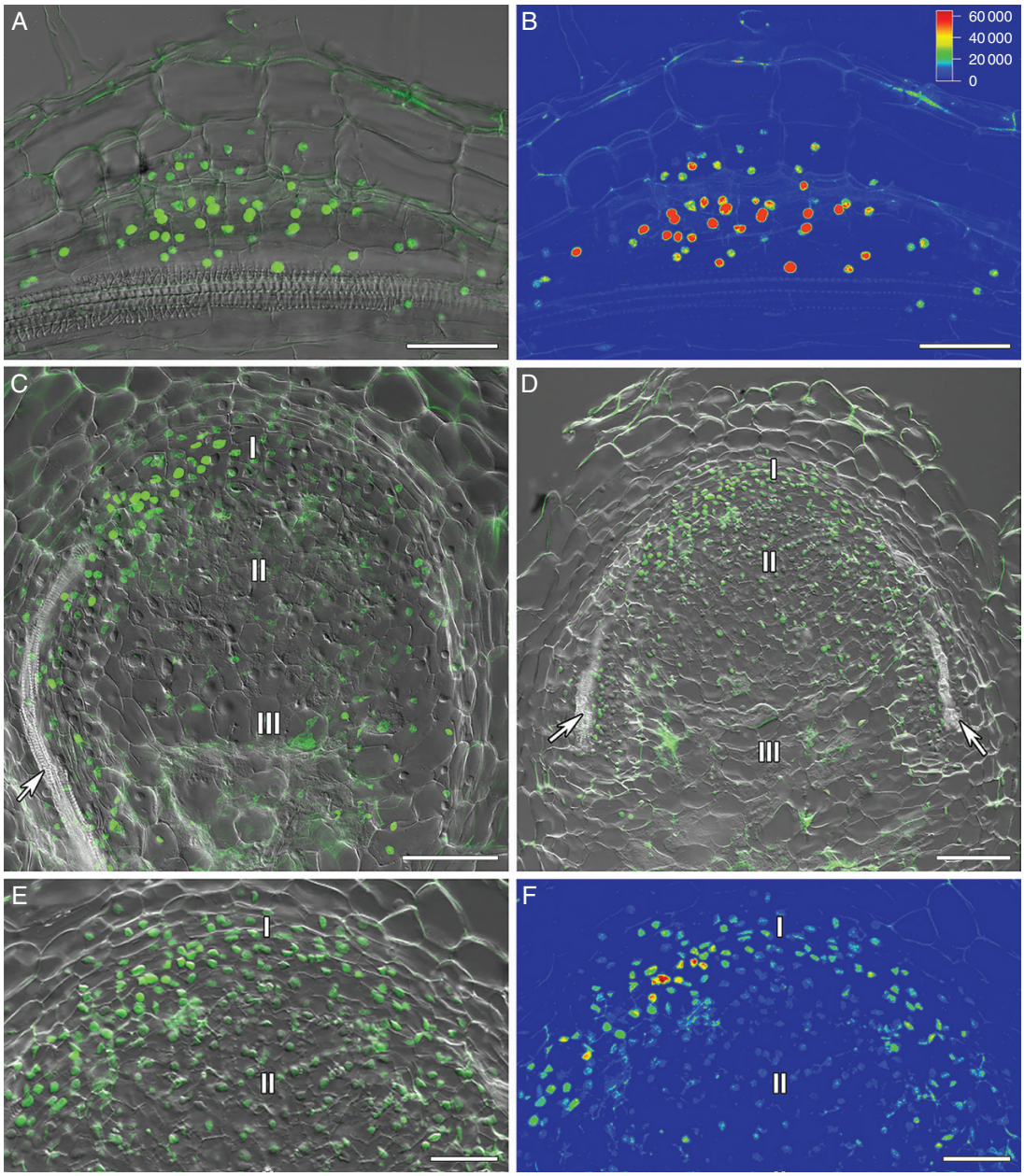

Fig. 1. Visualization of auxin response maxima in the nodule primordia and nodules of composite SGE pea wild-type plants containing the *DR5::GFP*-NLS construct. (A, B) Nodule primordium. (C) Two-week-old nodule. (D–F) Three-week-old nodules: (D) general view; (E, F) meristem. (A, C, D, E) Merge of differential interference contrast and green channel used for the *GFP*-NLS signal in green. (B, F) The heatmap shows colour-coded fluorescence signal intensities for the green signal channel; the quantification scale is the same for B and F images. I, meristem zone; II, infection zone; III, nitrogen fixation zone; arrows indicate vascular bundles. Scale bars are 50 µm (A, B, E, F) and 100 µm (C, D).

ipd3/*cyclops* mutants of legumes with the indeterminate nodule type has not been studied in detail. To investigate the cytokinin distribution in *sym33-2* and *sym33-3* mutants, the analysis was performed in composite pea plants. We found that the cytokinin distribution was significantly altered in the transgenic *sym33-2* and *sym33-3* mutants containing *pMtRR4::GUS*.

The distribution of the cytokinin response was reduced in the *sym33-2* and *sym33-3* mutants as compared with that in the wild-type line SGE (Fig. 3A). In 2-week-old nodules of *sym33-2* and *sym33-3*, the GUS reporter was detectable only in vascular tissues, and weak staining was associated with the meristem (Fig. 3B, C). Thus, the changes in the biosynthesis and distribution of cytokinins in the pea *sym33-2* and *sym33-3* mutants may be related to the disturbances in the development of symbiosis. In mutants impaired in the *Sym33* gene, due to the impaired infection process and the absence of release of bacteria from the infection threads (Tsyganov *et al.*, 1998; Voroshilova *et al.*, 2009; Tsyganova *et al.*, 2019), the differentiation of nodule tissue probably does not occur. Thus, cytokinins could be involved in differentiation control during the late stages of symbiosis development. At the same time, it could

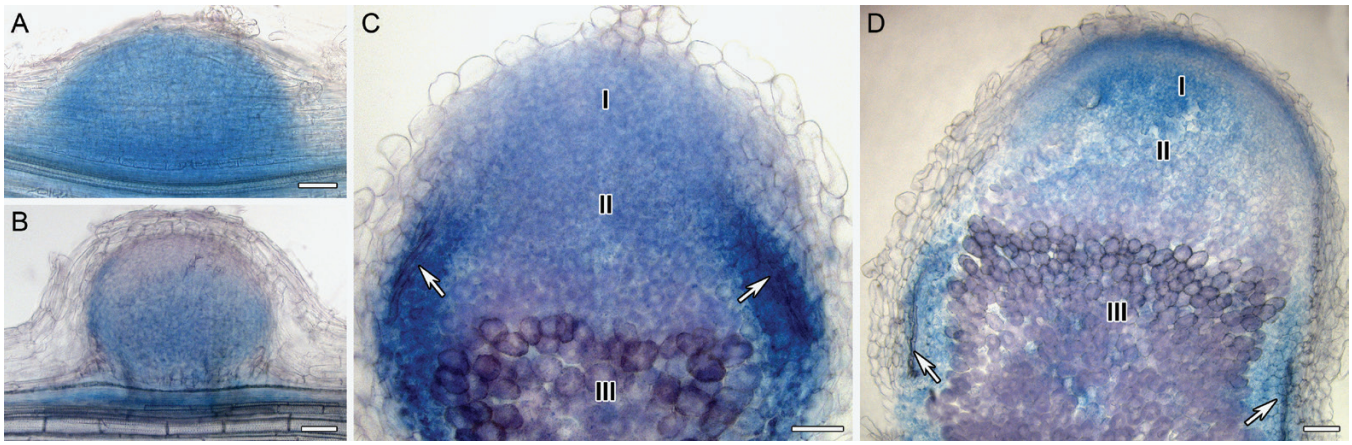

FIG. 2. Localization of *RR4* expression in pea nodule primordia and 2-week-old nodules expressing a *pMtRR4::GUS* genetic construct. (A, B) Nodule primordia; *pMtRR4::GUS* expression is visible in the pericycle and inner cortical cells of composite SGE pea wild-type plants. (C, D) Two-week-old pea nodules. Cytokinin response is stimulated in nodule primordia and in the meristem, infection zone and apical part of the nitrogen fixation zone of 2-week-old pea nodules. I, meristem zone; II, infection zone; III, nitrogen fixation zone; arrows indicate vascular bundles. Scale bars are 50 µm (A, B), 100 µm (C) and 75 µm (D).

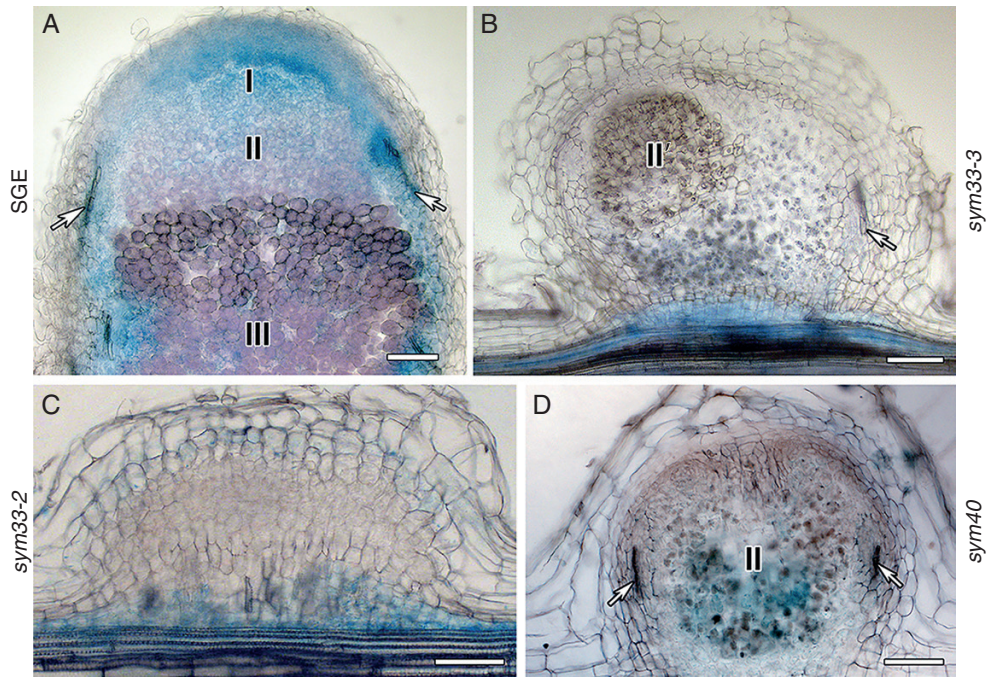

FIG. 3. Localization of *RR4* expression in pea nodules of the wild type and mutants expressing the *pMtRR4::GUS* construct 2 weeks after inoculation. (A) Two-week-old SGE pea nodules. (B) *sym33-3* mature nodule. *pMtRR4::GUS* expression is detected in peripheral tissues including vascular bundles. (C) *sym33-2* mature nodule. (D) *sym40*. I, meristem zone; II, infection zone; II', infection thread propagation zone; III, nitrogen fixation zone; arrows indicate vascular bundles. Scale bars are 100 µm (A, B, D) and 50 µm (C).

not be excluded that the level of bacteroid differentiation may affect cytokinin accumulation in the infected cells of nodules.

Distribution of cytokinins in the sym40 *mutant defective in the gene encoding the EFD transcription factor*

The pea *Sym40* gene is orthologous to the *M. truncatula EFD* gene (Nemankin, 2011). Analysis of mutants showed that the transcription factor EFD is required for the formation of functional nodules and essential for nodule differentiation in *M. truncatula* and pea (Tsyganov *et al.*, 1998; Vernié *et al.*, 2008; Voroshilova *et al.*, 2009). In addition, because the *M. truncatula efd* mutants and pea *sym40* mutant had more nodules, along with more frequent infection threads in the rhizodermis and root cortex, the EFD transcription factor may exert negative nodulation control (Vernié *et al.*, 2008; Voroshilova *et al.*, 2009).

In the transgenic *sym40* mutant, containing the *pMtRR4::GUS* construct, we detected a cytokinin response in the central part of the nodules where the release of bacteria occurred (Fig. 3D). This part can be described as the infection zone of the mutant,

although it significantly differed from the nodules of the wild-type line SGE. We concluded that the cytokinin accumulation in the central part of the nodule and the release of bacteria into the plant cells may be interconnected. The disturbances of differentiation processes in the *sym40* mutant (Voroshilova *et al.*, 2009) indicated that the cytokinins could play a role in regulating plant cell differentiation.

Immunolocalization of trans*-zeatin riboside and* N^6*-isopentenyladenosine in the wild type and mutants blocked at different stages of nodule development*

To further study the role of cytokinins in the differentiation of nodules and rhizobial cells, we assessed immunolocalization of *trans*-zeatin riboside and N^6-isopentenyladenosine, transport forms of cytokinins, in nodules of the wild type and the corresponding *sym33-3* and *sym40* mutants defective in the genes encoding the IPD3/CYCLOPS and EFD transcription factors.

In 2-week-old nodules of the wild-type line SGE (Fig. 4A–C), the anti-*trans*-zeatin riboside antibody signal was detected in the meristem (Fig. 5A–C), the infection zone and the proximal part of the nitrogen fixation zone. A similar pattern was observed for N^6-isopentenyladenosine in the 2-week-old nodules of the SGE wild type (Supplementary data Fig. S3A–C, G–I). These results were consistent with the data obtained with the cytokinin-responsive construct. In the early infection zone, *trans*-zeatin riboside was found in the plant cell cytoplasm but was absent in the infection threads and infection droplets (Fig. 5D–F). However, in the late infection zone and the proximal part of the nitrogen fixation zone, *trans*-zeatin riboside was present in the infection threads and infection droplets (Fig. 5G–I). The immunogold labelling of *trans*-zeatin riboside detected gold particles in the matrix of infection threads and in the exopolysaccharide capsule of bacteria (Fig. 6A). In these zones, the signal for *trans*-zeatin riboside was associated with the symbiosomes (Fig. 5D–L). The immunogold labelling confirmed the large amount of *trans*-zeatin riboside in symbiosomes, both in the peribacteroid space and within the bacteroids (Fig. 6C). Vesicles labelled with gold particles were associated with symbiosomes (Fig. 6B). In all zones, the signal for *trans*-zeatin riboside was not detected in the nuclei. In 4-week-old nodules of the SGE line (Supplementary data Fig. S4A–C), the signal intensity was much lower, especially in the nitrogen fixation zone. The immunogold labelling showed low amounts of *trans*-zeatin riboside in senescent symbiosomes (Fig. 6D).

Two-week-old nodules of the *sym33-3* mutant forming nodules with 'locked' infection threads (Tsyganov *et al.*, 1998) exhibited a maximal amount of *trans*-zeatin riboside in the meristem (Fig. 4D–F). The *trans*-zeatin riboside was absent in the 'locked' infection threads but present in the nuclei and cytoplasm of colonized cells (Fig. 7A–C) and in the infection droplets (Fig. 7D–F), which are occasionally formed (Tsyganov *et al.*, 2011). A similar pattern was observed for N^6-isopentenyladenosine (Supplementary data Fig. S3D–F, J–L). In 4-week-old nodules, the signal for *trans*-zeatin riboside was limited to the meristem (Supplementary data Fig. S4D–F).

Although the signal distribution patterns of *trans*-zeatin riboside and N^6-isopentenyladenosine were similar in the nodules of SGE wild type and *sym33-3* mutants, *trans*-zeatin riboside had a higher labelling intensity than N^6-isopentenyladenosine. Thus, only *trans*-zeatin riboside labelling was used in the analysis of other genotypes.

In 2-week-old nodules of the *sym40* mutant forming nodules with abnormal histological organization, hypertrophied infection droplets and abnormal bacteroids (Tsyganov *et al.*, 1998), the maximum signal for *trans*-zeatin riboside was detected in the meristem (Fig. 4G–I) and in infected cells (Figs 4G–I and 7G–I). In contrast to wild-type nodules, the nuclei had accumulated large amounts of *trans*-zeatin riboside (Fig. 7G–L), while the hypertrophied infection droplets were free from the signal (Fig. 7G–L). In 4-week-old nodules of the *sym40* mutant, the signal intensity for *trans*-zeatin riboside was reduced (Supplementary data Fig. S4G–I) as in the wild-type nodules.

Along with the *sym33-3* and *sym40* ineffective mutants, two other mutants, the *sym26* mutant forming nodules with morphologically differentiated bacteroids and premature degradation of symbiotic structures (Serova *et al.*, 2018) and the *sym31* mutant forming nodules with undifferentiated bacteroids (Borisov *et al.*, 1997), were used. In the 2-week-old nodules of the *sym26* mutant that typically form nodules with morphologically differentiated bacteroids undergoing premature degradation (Serova *et al.*, 2018), the distribution of *trans*-zeatin riboside was similar to that in the wild-type nodules (Fig. 4J–L). However, in mutant nodules, the respective signals were detected in the nuclei (Fig. 8G–L). In 4-week-old nodules, the *trans*-zeatin riboside level was dramatically reduced (Supplementary Fig. S4J–L). These results further confirmed that cytokinins are involved in the infection process in mature nodules and in the nodule tissue and bacteroid differentiation.

In the 2-week-old nodules of *sym31* mutants that typically form nodules with undifferentiated bacteroids (Borisov *et al.*, 1997), the strongest *trans*-zeatin riboside signal was observed in the meristem and the infection zone, but the signal intensity was decreased in the zone that corresponded to the nitrogen fixation zone in the wild type (Supplementary data Fig. S5D–F). In the infected cells of *sym31* mutants, the signal intensity was significantly lower (Fig. 8D–F) than that in the Sprint-2 wild type (Fig. 8A–C). In 4-week-old nodules, the *trans*-zeatin riboside level was sharply decreased (Supplementary data Fig. S5J–L).

Expression of cytokinin metabolic genes ISOPENTENYL TRANSFERASE *(*IPT*) and* LONELY GUY *(*LOG*) in pea wild type and mutants*

To elucidate the basis for the changes in the hormone level in developing nodules, we profiled the expression of plant genes controlling the metabolism of these phytohormones, as well as the primary response. In accordance with our previous results for other pea cultivars, the expression levels of *LOG1*, *IPT1*, *IPT3*, *IPT4* and A-type response regulators *RR8* and *RR11* were up-regulated noticeably in the nodules of pea SGE wild type (Azarakhsh *et al.*, 2015; Dolgikh *et al.*, 2017). In contrast, in the 2-week-old nodules of *sym33-2* and *sym33-3* mutants, the expression levels of *LOG1* and *RR11* were significantly reduced (Fig. 9A, B). The expression levels of *IPT3* and *RR8* were also decreased as compared with those in the wild-type nodules, while the levels of *IPT1* and *IPT4* did not change significantly. A similar pattern was found in the mature 3-week-old nodules

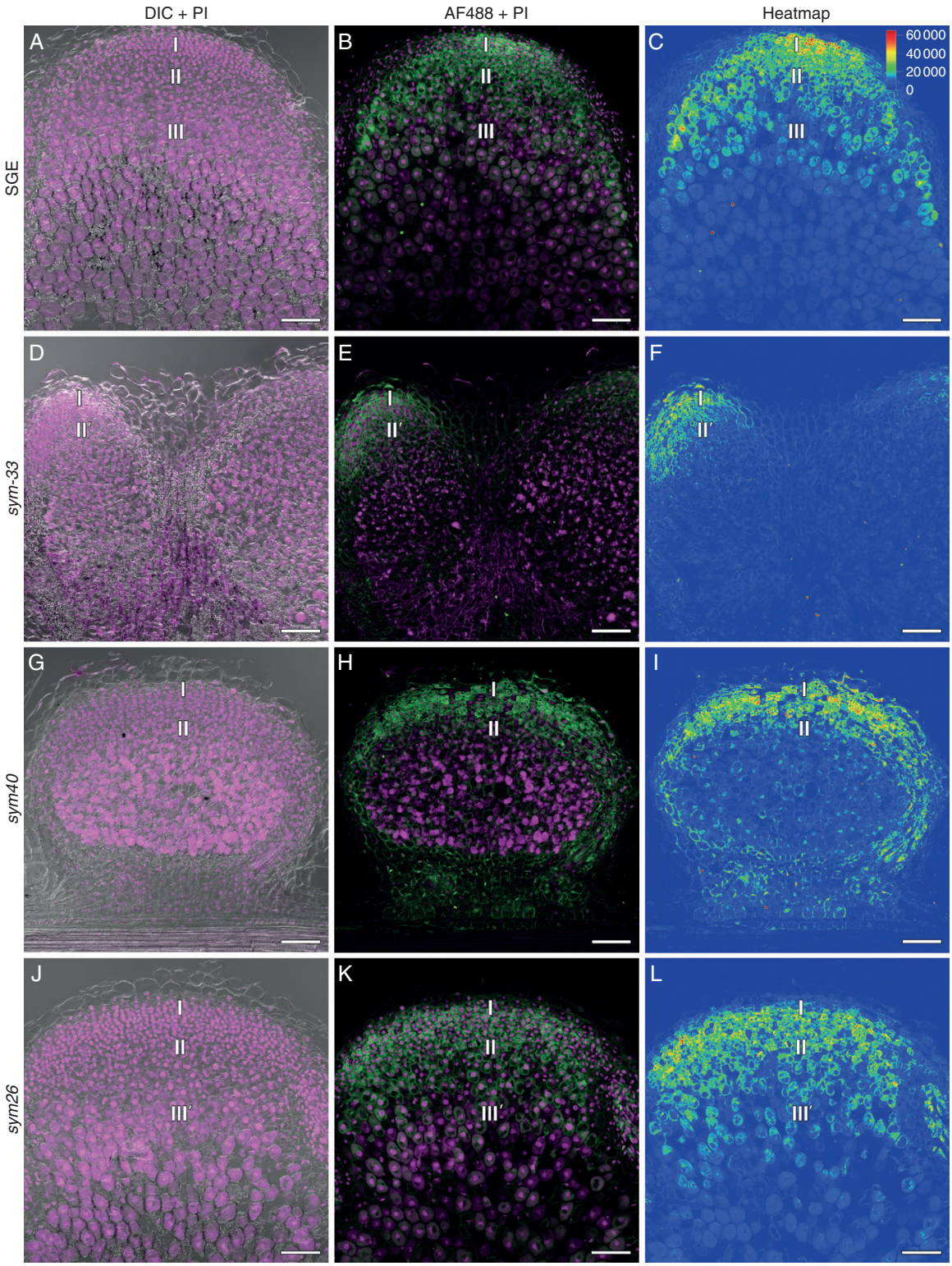

FIG. 4. Immunolocalization of *trans*-zeatin riboside in the 2-week-old nodules of pea SGE wild type and corresponding mutants, general view. (A–C) SGE. (D–F) *sym33-3*. (G–I) *sym40*. (J–L) *sym26*. (A, D, G, J) Merge of differential interference contrast (DIC) and magenta channel. (B, E, H, K) Merge of green and magenta channels. A single optical section is presented: *trans*-zeatin riboside in green and DNA (bacteria and nuclei) in magenta. (C, F, I, L) The heatmap shows colour-coded fluorescence signal intensities for the green signal channel; the quantification scale is the same for all images. PI, propidium iodide; AF488, Alexa Fluor 488. I, meristem zone; II, infection zone; II', infection thread propagation zone; III, nitrogen fixation zone; III', zone corresponding to the nitrogen fixation zone of wild-type nodules. Scale bars are 100 µm.

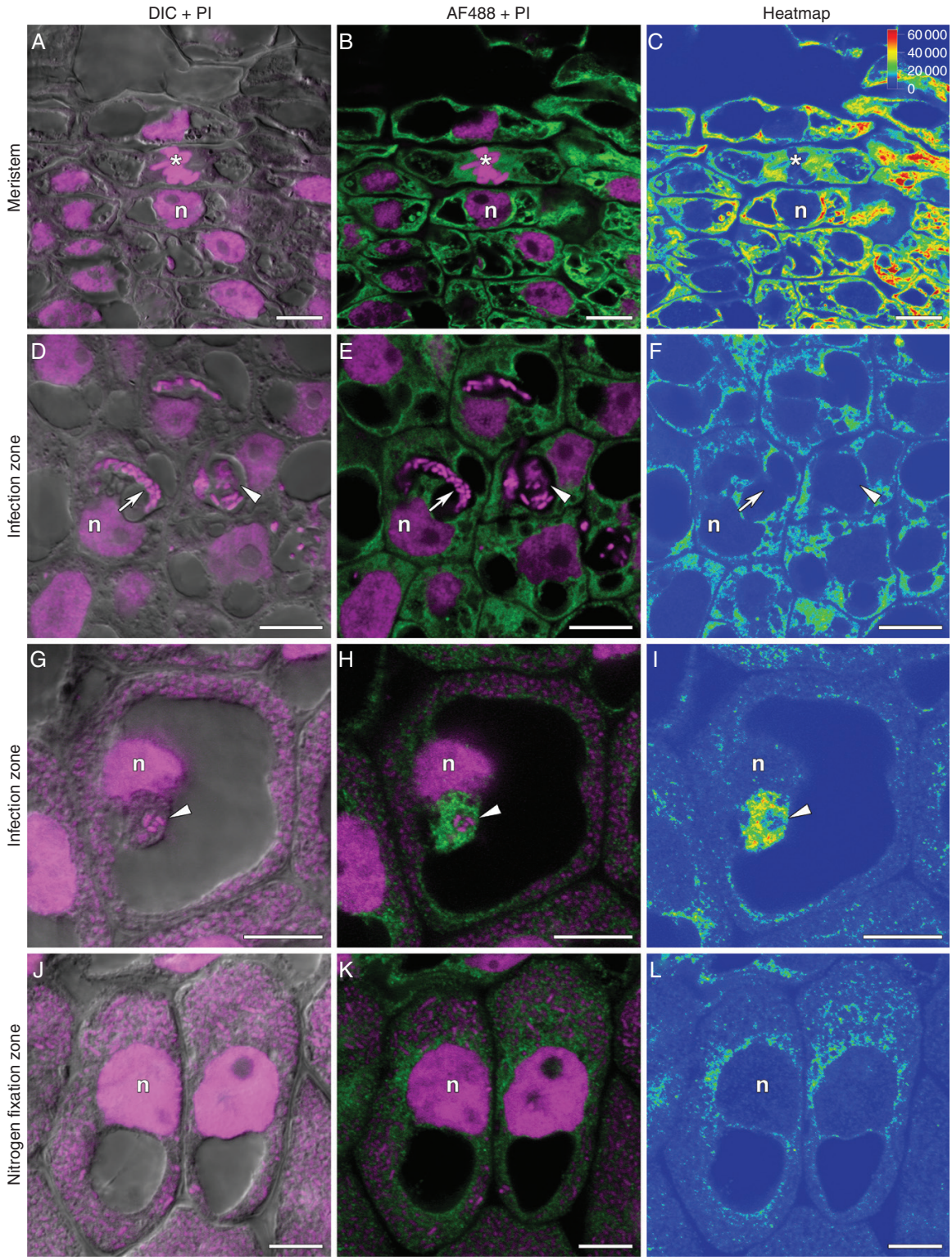

FIG. 5. Immunolocalization of *trans*-zeatin riboside in the 2-week-old nodules of pea SGE wild type. (A–C) Meristem. (D–F) Cells from the early infection zone. (G–I) Cells from the late infection zone. (J–L) Cells from the nitrogen fixation zone. (A, D, G, J) Merge of differential interference contrast (DIC) and magenta channel. (B, E, H, K) Merge of green and magenta channels. A single optical section is presented: *trans*-zeatin riboside in green and DNA (bacteria and nuclei) in magenta. (C, F, I, L) The heatmap shows colour-coded fluorescence signal intensities for the green signal channel; the quantification scale is the same for all images. PI, propidium iodide; AF488, Alexa Fluor 488. n, nucleus; *, mitosis; arrows indicate infection threads; arrowheads indicate infection droplets. Scale bars are 10 µm.

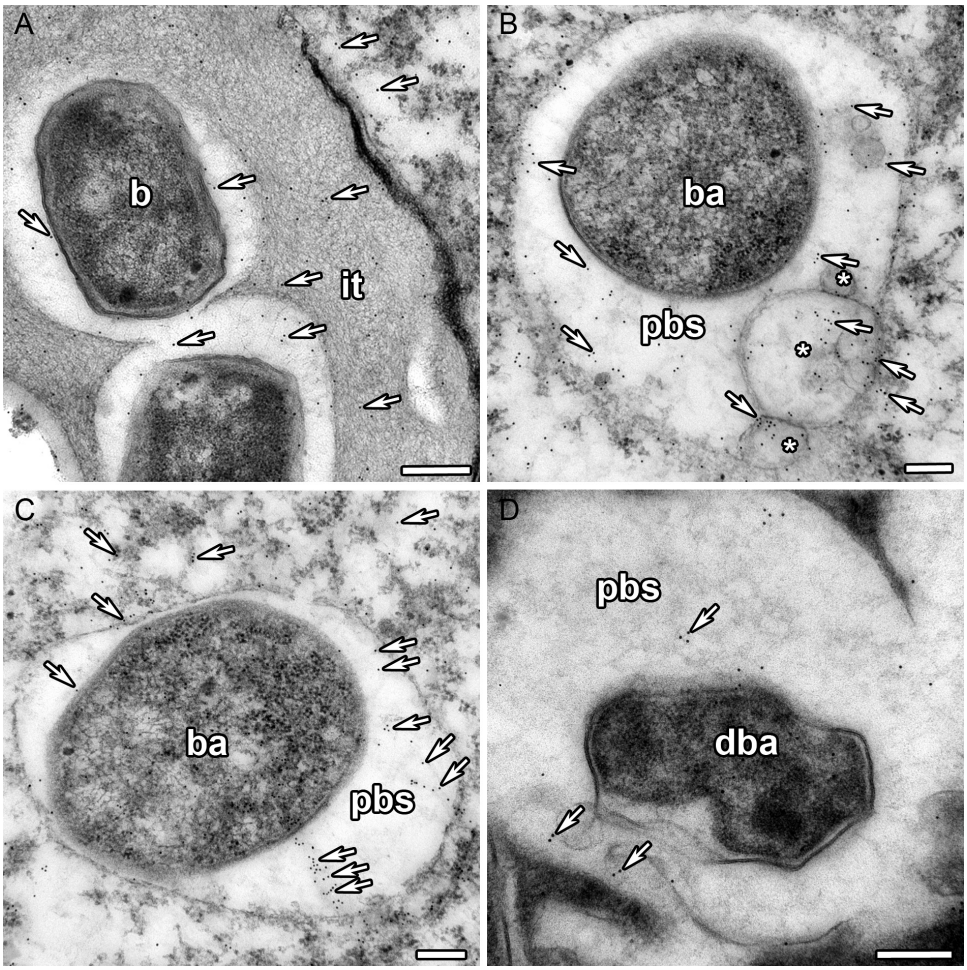

FIG. 6. Immunogold localization of *trans*-zeatin riboside in the 2-week-old nodules of pea SGE wild type. (A) Infection thread. (B) Symbiosome with vesicles labelled with gold particles. (C) Mature symbiosome. (D) Degrading symbiosome. it, infection thread; b, bacterium; ba, bacteroid; pbs, peribacteroid space; dba, degrading bacteroid; *, vesicle; arrows indicate gold particles. Scale bars are 250 nm (A) and 200 nm (B–D).

of these mutants (Supplementary data Fig. S6). In mutants defective in the *sym33* gene, the nodules remained uninfected because they contain 'locked' infection threads without bacterial release into the cytoplasm of the plant cells (Tsyganov *et al.*, 1998; Tsyganova *et al.*, 2019). These observations suggested that stimulation of cytokinin biosynthesis and additional activation of the cytokinin receptor in pea nodules may be associated with the release of bacteria from infection threads and subsequent plant cell differentiation (Fig. 9A, B).

To test this assumption, we also conducted an analysis of the *sym40* pea mutant, in which the infection process and differentiation were impaired. In the nodules of this mutant, the hypertrophic infection threads were formed but the release of bacteria from the infection threads occurred with a delay (Tsyganov *et al.*, 1998; Voroshilova *et al.*, 2009). In contrast to the *sym33-2* and *sym33-3* mutants, an increase of *LOG1*, *IPT3*, *RR8* and *RR11* gene expression was detected in the nodules of the *sym40* mutant (Fig. 9A, B), where the infection of the nodules occurred, but subsequent stages of plant cell and bacteroid differentiation were impaired. This indicated a link between the activation of these genes and certain stages of nodule development.

The balance between cell proliferation and differentiation may be controlled by cell cycle regulators. The transition of cells to endoreduplication may be linked to the expression of *CCS52A* (Takahashi *et al.*, 2013). In contrast to the wild type and the *sym40* mutant, we were not able to detect an increase in the level of *CCS52A* in the nodules of *sym33-2* and *sym33-3* mutants (Fig. 9A, B).

It has been shown that the KNOX3 transcription factor may be involved in the upregulation of *LOG* and *IPT* genes in pea (Azarakhsh *et al.*, 2015). In addition, the NIN transcription factor is known to induce the expression of the cytokinin receptor CRE1 in cortical cells (Vernié *et al.*, 2015). In our experiments, the expression of *KNOX3* and *NIN* was significantly stimulated in the 2-week-old nodules of the SGE wild type and *sym40* mutant, but not in *sym33-2* and *sym33-3* mutants (Fig. 9A, B). The decreased level of *KNOX3* expression in *sym33* mutants was also found previously (Dolgikh *et al.*, 2019). These observations suggested that the KNOX3 and NIN transcription factors were involved in promoting the accumulation of cytokinins in pea nodules.

Previous studies in legume plants have shown that the transcription factor EFD is required for the formation of functional nodules and essential for nodule differentiation (Vernié *et al.*, 2008). In our experiments, we were not able to detect an increased *EFD* level in the nodules of *sym33-2* and *sym33-3*

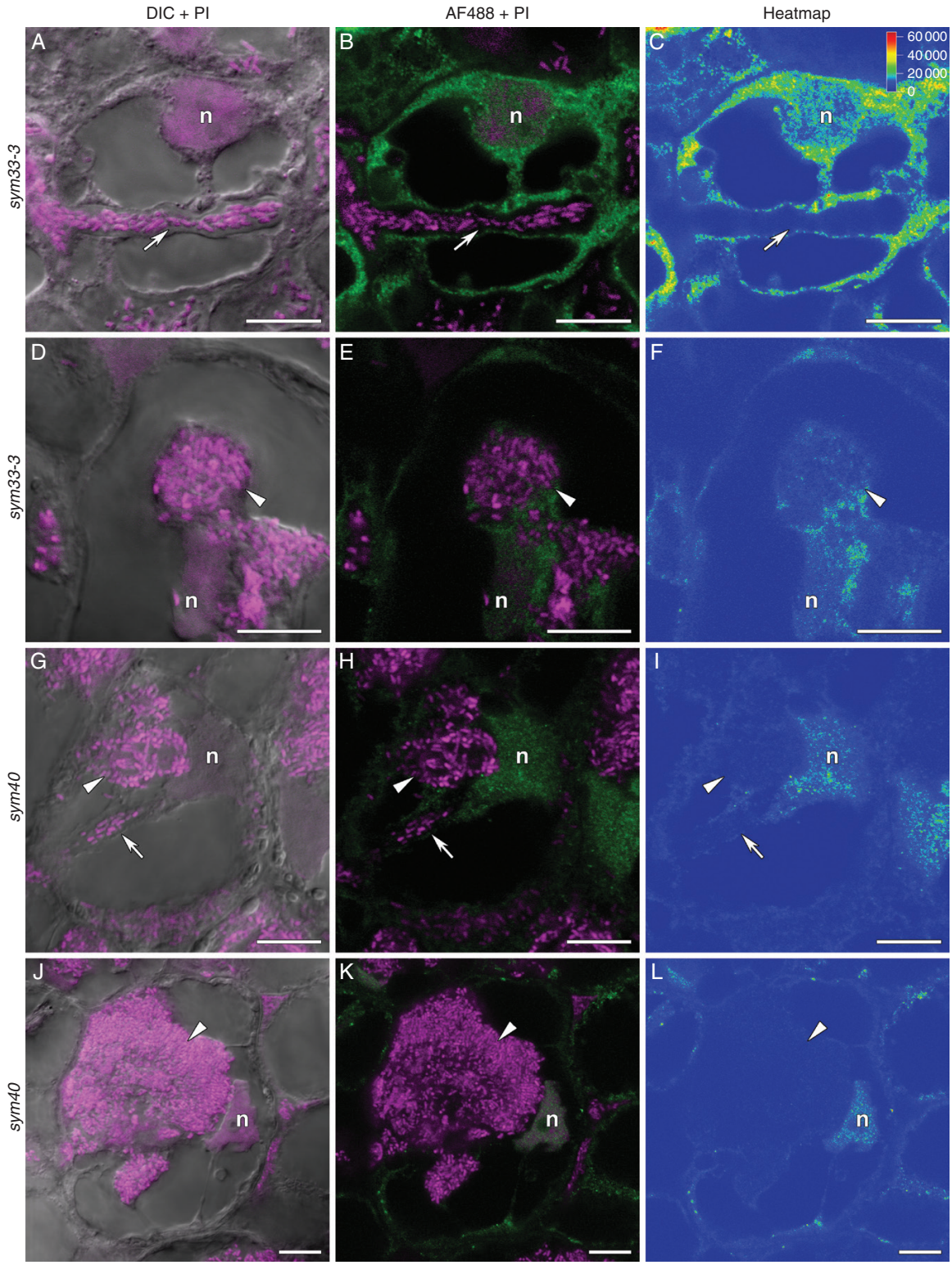

FIG. 7. Immunolocalization of *trans*-zeatin riboside in 2-week-old nodules of pea mutants *sym33-3* (A–F) and *sym40* (G–L). (A–C) Colonized cell with a 'locked' infection thread. (D–F) Colonized cell with an infection droplet. (G–I) Recently infected cell with an infection droplet. (J–L) Colonized cell with a hypertrophied infection droplet. (A, D, G, J) Merge of differential interference contrast (DIC) and magenta channel. (B, E, H, K) Merge of green and magenta channels. A single optical section is presented: *trans*-zeatin riboside in green and DNA (bacteria and nuclei) in magenta. (C, F, I, L) The heatmap shows colour-coded fluorescence signal intensities for the green signal channel; the quantification scale is the same for all images. PI, propidium iodide; AF488, Alexa Fluor 488. n, nucleus; arrows indicate infection threads; arrowheads indicate infection droplets. Scale bars are 10 µm.

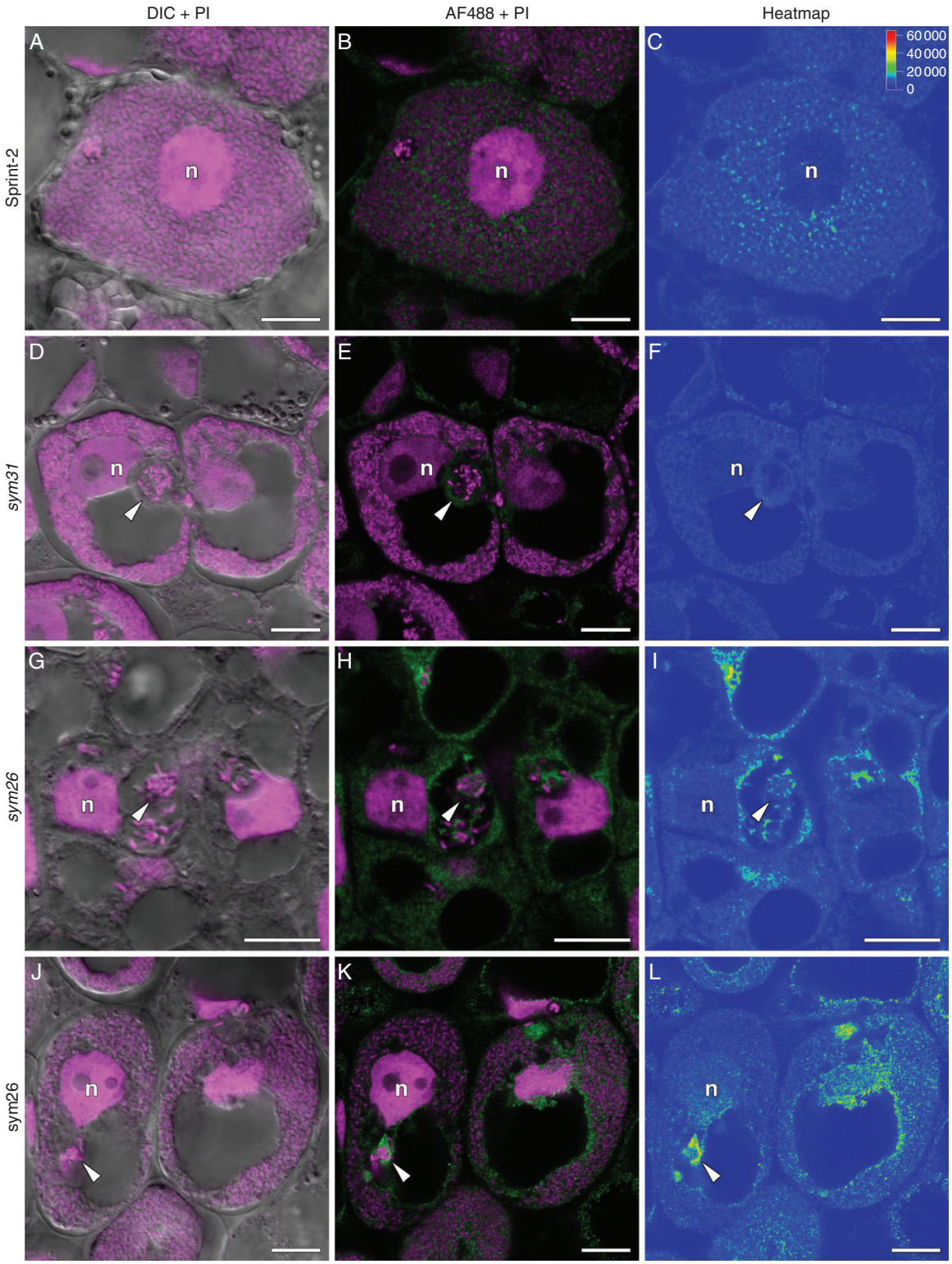

FIG. 8. Immunolocalization of *trans*-zeatin riboside in 2-week-old nodules of pea Sprint-2 wild type (A–C), corresponding *sym31* mutant (D–F) and *sym26* mutant (G–L). (A–C) Infected cell from the nitrogen fixation zone. (D–F) Infected cell from the zone corresponding to the nitrogen fixation zone. (G–I) Recently infected cell with an infection thread and droplet. (J–L) Infected cell from the zone corresponding to the nitrogen fixation zone. (A, D, G, J) Merge of differential interference contrast (DIC) and magenta channel. (B, E, H, K) Merge of green and magenta channels. A single optical section is presented: *trans*-zeatin riboside in green and DNA (bacteria and nuclei) in magenta. (C, F, I, L) The heatmap shows colour-coded fluorescence signal intensities for the green signal channel; the quantification scale is the same for all images. PI, propidium iodide; AF488, Alexa Fluor 488. n, nucleus; arrowheads indicate infection droplets. Scale bars are 10 µm.

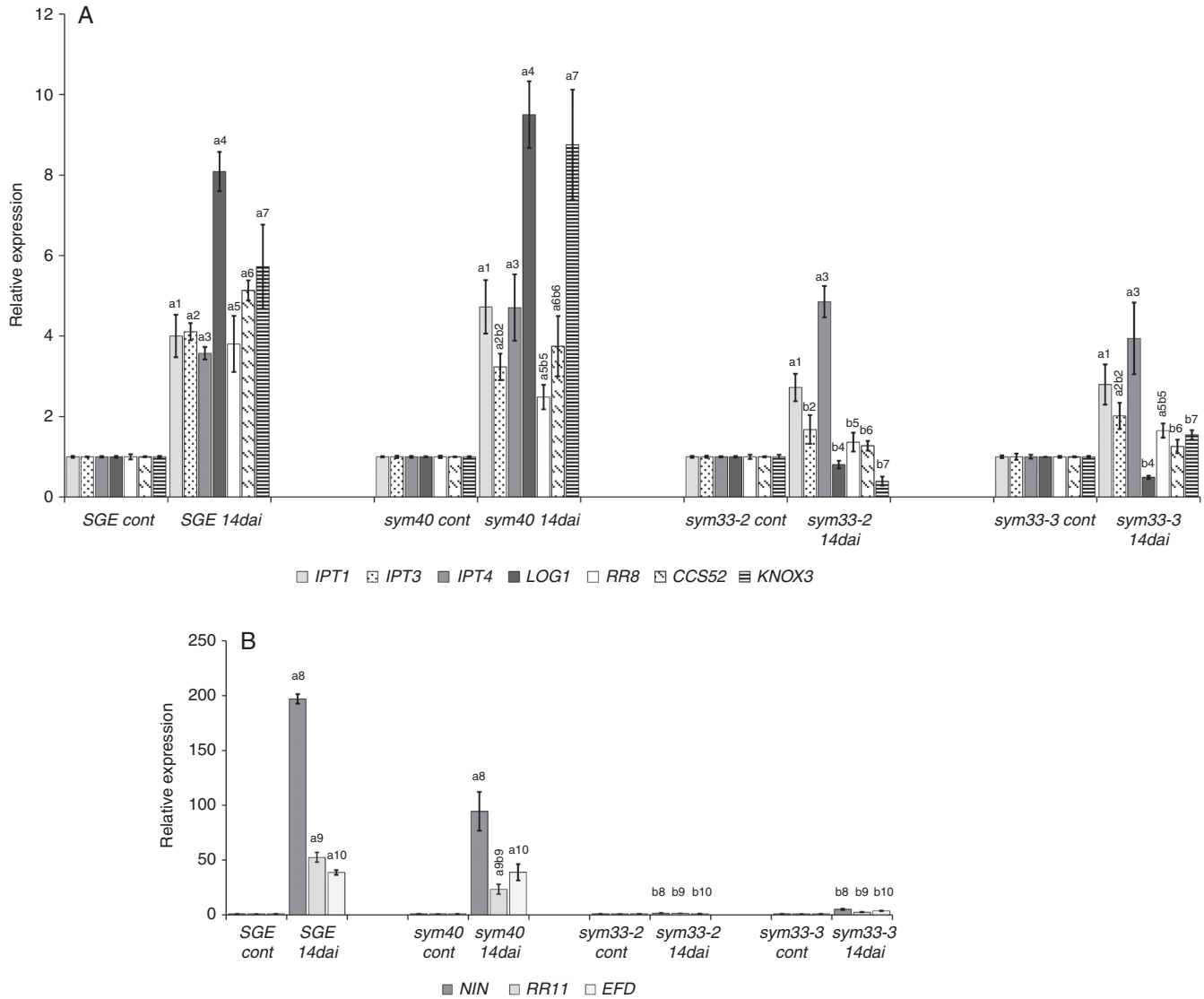

FIG. 9. Expression pattern of cytokinin metabolic and regulatory genes *IPT1*, *IPT3*, *IPT4*, *LOG1*, *RR8*, *CCS52A* and *KNOX3* (A), and *NIN*, *RR11* and *EFD* (B) in pea wild type and *sym33-2*, *sym33-3* and *sym40* mutants 2 weeks after inoculation (14 dai). Transcript levels of genes were normalized against pea *Ubiquitin* and *Actin* genes. For each gene, the transcript level in non-inoculated roots of the wild type or mutants was set to 1 (control), and the level in nodules of the inoculated wild type or mutants was calculated relative to the control values. The graphs show the results of three independent experiments. The error bars represent the s.e.m. of three repeats. To conduct one biological repeat, the fragments of non-inoculated main roots or nodules from 3–4 plants were collected and used to isolate RNA. Pairwise comparisons were made using Dunn's test, and the CLD algorithm was performed to summarize the sets of groups that differed significantly for each gene (groups are shown with different letters on the histogram). Kruskal–Wallis one-way analysis of variance showed significant differences in expression of genes *IPT3* [H(d.f. = 3) = 9.59, $P = 0.022$], *LOG1* [H(d.f. = 3) = 10.17, $P = 0.017$], *RR8* [H(d.f. = 3) = 10.42, $P = 0.015$], *KNOX3* [H(d.f. = 3) = 11.18, $P = 0.011$], *NIN* [H(d.f. = 3) = 11.36, $P = 0.0099$], *EFD* [H(d.f. = 3) = 9.56, $P = 0.023$] and *RR11* [H(d.f. = 3) = 10.51, $P = 0.015$] depending on the type of plant.

mutants in contrast to the wild type (Fig. 9A, B). These observations suggested that activation of EFD in the wild type may be associated with the subsequent nodule differentiation.

DISCUSSION

In addition to studying the well-established function of cytokinin and auxin in the initiation of nodule formation (for a recent review, see Gamas *et al.*, 2017), in this study, we have investigated the effect of these phytohormones on other aspects of nodulation. In 2- and 3-week-old pea nodules, the response to auxin was localized in the meristem, bordering cells around vascular bundles and peripheral tissues. Similar localization patterns have been reported in the nodules of other legumes, such as *L. japonicus, Trifolium repens* and *G. max* (Mathesius *et al.*, 1998; Suzaki *et al.*, 2012; Fisher *et al.*, 2018). This pattern may indicate a critical role for auxin in maintaining the meristem and functioning of the vasculature. A previous report indicated that 2- and 3-week-old pea nodules had maximal cytokinin levels in the meristem and infection zone, and 4-week-old nodules maintained a similar level of cytokinins in the meristem but showed significantly reduced levels in the infection zone (Syōno *et al.*, 1976). Owing to the correlation between the decrease in cytokinin levels with age of the

nodules and the decrease in their meristematic activity, it has been suggested that cytokinins affect nodule morphogenesis by regulating the mitotic activity of the nodule meristem (Syōno *et al.*, 1976). In our experiments, we used reporter constructs and assessed the immunolocalization of *trans*-zeatin riboside and N^6-isopentenyladenosine in 2- and 4-week-old wild-type pea nodules and found that the cytokinin distribution profile resembled the previously described pattern (Fig. 10). We propose that in addition to the localization of cytokinins in the meristem of wild-type nodules, their presence in the infection zone and apical part of the nitrogen fixation zone supports a potential role for cytokinins in the control of intracellular bacterial accommodation and tissue differentiation. The first experimental evidence for this assumption was obtained using *M. truncatula*, a legume with a similar nodulation type, demonstrating that the *M. truncatula cre1* mutant defective in cytokinin perception displayed significantly disturbed zonation and tissue differentiation in rarely appearing nodules (Plet *et al.*, 2011). In *Arachis hypogaea*, switching off *AhHK1* encoding cytokinin receptor histidine-kinase1 led to the formation of undifferentiated nodules associated with the proliferation of infected cells (Kundu and DasGupta, 2017). To study the potential role of cytokinins in nodulation regulation, we performed a detailed analysis using pea ineffective mutants impaired in the genes encoding IPD3/CYCLOPS and EFD transcription factors.

Altered patterns of cytokinin response and immunolocalization in sym33 *and* sym40 *mutants defective in IPD3/CYCLOPS and EFD transcription factors, respectively, indicate their involvement in the control of the late stages of symbiosis*

In this study, we found altered patterns of cytokinin response and immunolocalization in *sym33* and *sym40* mutants defective in IPD3/CYCLOPS and EFD transcription factors, respectively. In *sym33* mutants, the cytokinin localization area was mostly limited to the meristem, whereas cytokinins were absent in the central part of non-infected nodules (Fig. 10B). In contrast, in the *sym40* mutant, cytokinins were detected in the infection zone, where the bacteria are released into the cytoplasm of plant cells (Fig. 10C). However, the bacterial release into plant cells was delayed in this mutant. Therefore, the enhanced cytokinin accumulation during the late stages of symbiosis development may be linked to bacterial penetration into the plant cells and subsequent plant cell differentiation. The interconnection between cytokinin regulation and bacterial release has been previously suggested (Held *et al.*, 2014). Indeed, in the *L. japonicus lhk1* mutant, the delayed formation of rare nodules was completely abolished by this mutation that prevented bacterial entry (Held *et al.*, 2014).

In legumes with indeterminate nodule type, the primary cytokinin accumulation occurred in the rhizodermis (root hairs) and later in the cells of developing primordia (Lohar *et al.*, 2004; Op den Camp *et al.*, 2011; Jardinaud *et al.*, 2016). The *sym33* mutants developed a reduced number of nodule primordia due to an impaired infection process, and these nodule primordia remained uninfected because the infection threads grew only in the outer cortex and did not penetrate the primordia (Voroshilova *et al.*, 2009). In contrast, co-ordinated infection

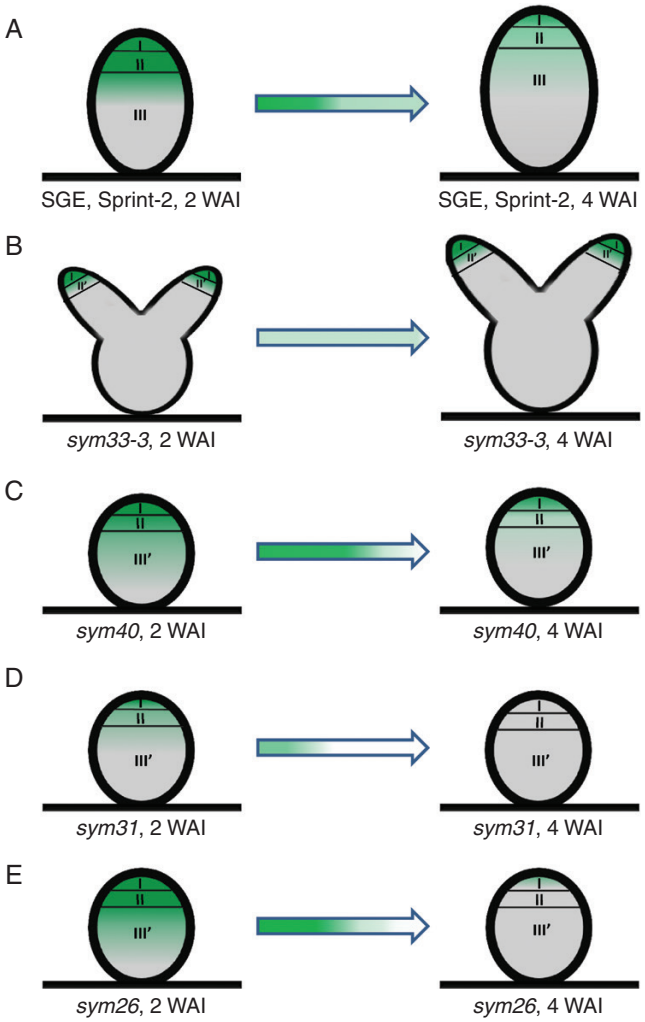

Fig. 10. Scheme of cytokinin localization in nodules of the wild type (A) and mutants *sym33-3* (B), *sym40* (C), *sym31* (D) and *sym26* (E) at 2 and 4 weeks after inoculation (WAI). Zones of the nodule are designated by Roman numerals: I, meristem; II, infection zone; II', infection thread propagation zone; III, fixation zone; and III', zone corresponding to the nitrogen fixation zone in the wild type. A decrease in the colour intensity of the arrow indicates a reduction in cytokinin levels.

thread development and nodule organogenesis occurred in the *sym40* mutant, and infection threads penetrated the nodule primordia (Voroshilova *et al.*, 2009). These observations indicated a co-ordinated signal exchange between the rhizodermis and the cortical layers during nodule development in the *sym40* mutant but not in the *sym33* mutants.

Role of the NIN and KNOX3 transcription factors in the regulation of late stages of nodulation

Potential candidates for regulators that perform such non-cell-autonomous functions are transcription factors that are activated in response to Nod factor exposure in the rhizodermis and may be translocated into cortical cells. Indeed, in the nodules of the *sym33* mutants, the expression levels of genes encoding the NIN and KNOX3 transcription factors were significantly

reduced. Owing to the involvement of IPD3/CYCLOPS in the transcription activation of NIN (Singh *et al.*, 2014) and its potential translocation into the cortical cells (Vernié *et al.*, 2015), the mutations in the *Sym33* gene may interrupt a co-ordinated signal exchange between tissue layers. In this study, we also showed a possible link between the IPD3/CYCLOPS transcription factor and KNOX3 activation. As previously reported, the KNOX transcription factors perform non-cell-autonomous functions in plants (Hake *et al.*, 2004). This suggests that KNOX3 may play a critical role in the signal exchange between the rhizodermis and the cortical layers during the early stages of symbiosis development. However, this suggestion needs to be verified in further investigations.

The lack of cytokinins in the central part of nodules in the *sym33* mutants defective in bacterial accommodation demonstrates that regulators controlled by the IPD3/CYCLOPS transcription factor may be involved in signal transduction that triggers secondary cytokinin accumulation in nodules. Previously, the involvement of the KNOX3 transcription factor in activating genes required for cytokinin biosynthesis regulation has been confirmed in pea and *M. truncatula* (Azarakhsh *et al.*, 2015; Di Giacomo *et al.*, 2017). Based on this finding, we used pea mutants to examine the expression of crucial genes controlling cytokinin biosynthesis and response. Decreased expression levels of *LOG1* and *IPT3*, along with those of *RR8* and *RR11*, in the *sym33* mutants may represent further evidence that KNOX3 acts during the late stages of nodule development and in the active nodule. It is interesting to note that the NIN transcription factor can stimulate *CRE1* expression in cortical cells during nodule formation (Vernié *et al.*, 2015). In addition, the *NIN* expression may be dependent on the cytokinins, because cytokinin response elements have been found in the *NIN* promoter region (Liu *et al.*, 2018). Therefore, activation of *KNOX3* and *NIN* expression during the late nodulation stages may be linked to cytokinin accumulation and perception in the infection zone and apical part of the nitrogen fixation zone. At the current stage of research, the analysis of infection-impaired pea mutants revealed the relationship among *NIN* and *KNOX3* activation, bacterial release and cytokinin accumulation in nodules. The bacterial release and continued Nod factor production in bacteroids may be important for cytokinin biosynthesis stimulation. However, this assumption requires further investigation. Which processes can be potentially regulated by these cytokinins?

Influence of cytokinins on plant cell differentiation

Recent studies identified legume mutants defective in the genes necessary to control endoreduplication, which is related to the process of tissue differentiation during nodule formation (Suzaki *et al.*, 2014; Yoon *et al.*, 2014). Since the transition of cells to endoreduplication can be directly controlled by cytokinins, as demonstrated in arabidopsis (Takahashi *et al.*, 2013), the cytokinins in legumes may affect tissue differentiation during nodule development. To test this hypothesis, we performed an expression analysis of *CCS52A* in *sym33* and *sym40* mutants. We failed to detect *CCS52A* upregulation in *sym33* mutants, suggesting a link between cytokinins and endoreduplication control. Some *CCS52A* expression was detected in the *sym40* mutant but it was not as pronounced as that in the wild-type pea, indicating an association with the tissue differentiation defects in the mutant (Voroshilova *et al.*, 2009). The impaired differentiation in *sym33* mutants corresponded to a reduced expression level of the gene encoding the EFD transcription factor that acts during the late stages of nodule development. This implies that regulation of plant tissue differentiation involving cytokinins, CCS52A and EFD is required for the formation of functional nitrogen-fixing nodules.

The underlying mechanism for the participation of phytohormones in cell differentiation in nodule tissues has yet to be elucidated, but a detailed analysis of this regulation has been performed on the roots of the model plant arabidopsis. Importantly, cytokinins are involved in regulating the root system architecture. In the parental root meristem, cytokinin signalling ensures the balance between cell proliferation and differentiation (Ioio *et al.*, 2007; Moubayidin *et al.*, 2010). Cytokinins control the cell differentiation rate by negatively regulating the positive effect of auxin on cell proliferation. In the arabidopsis main root meristem, cytokinins, via the receptor AHK3 and B-type response regulators ARR1 and ARR12, directly activate the transcription of SHY2/IAA3, a member of the Aux/IAA family of auxin signalling repressors (Ioio *et al.*, 2007, 2008). Since SHY2/IAA3 negatively regulates PIN expression, its activation results in limiting auxin transport and allows cell differentiation in the root transition zone (Ioio *et al.*, 2008). In addition, the cytokinin-activated B-type response regulator ARR2 directly upregulates the expression of *CCS52A1*, which encodes an activator of an E3 ubiquitin ligase, also described as the anaphase-promoting complex/cyclosome, mediating degradation of cell cycle regulators. It co-ordinates root growth by promoting endoreduplication and restricting cell proliferation in the root meristem.

Furthermore, cytokinins act as negative regulators of the lateral root initiation (Laplaze *et al.*, 2007), and the downregulation of their accumulation allowed the specification of lateral root founder cells (Bielach *et al.*, 2012). In the pericycle cells between the existing lateral root primordia, cytokinins negatively control lateral root initiation by reducing the expression of the auxin efflux carrier PIN, thus preventing the establishment of the auxin maximum (Del Bianco *et al.*, 2013). Similar mechanisms may be involved in regulating nodule formation. If synthesized under Nod factor control, cytokinins negatively regulate *PIN* expression in the root cortex, which enhances local auxin accumulation (Plet *et al.*, 2011). Therefore, cytokinin-dependent regulation of the auxin response maximum occurs during the initiation of symbiosis development that stimulates local cell proliferation, which suggests a common mechanism for regulating the development of roots and nodules. However, the exact role of cytokinins during the late stages of nodulation associated with plant cell and bacteroid differentiation remains to be elucidated.

Effect of sub-cellular localization of cytokinins

We observed an unusually strong accumulation of *trans*-zeatin riboside in the nuclei of *sym33-3*, *sym40* and *sym26* mutants, whereas the *trans*-zeatin riboside signal was almost

absent in the nuclei of cells from different histological nodule zones in the SGE and Sprint-2 wild-type lines, as well as in the *sym31* mutants. This indicated that *sym33-3*, *sym40* and *sym26* affected the cellular transport of *trans*-zeatin riboside. Previously, different cytokinin forms have been detected in the nuclei of somatic and zygotic embryos of *Tilia cordata* (Kärkönen and Simola, 1999) and somatic embryos of *Dactylis glomerata* (Ivanova *et al.*, 1994). However, the precise function of cytokinins in the nuclei merits further investigation.

Cytokinins negatively regulate infection thread and infection droplet development in nodules

In contrast to the positive effect that cytokinins exert on nodule organogenesis, they have a negative impact on rhizobial infection, as demonstrated by the *Ljlhk1-1* mutant with a manifested hyperinfection phenotype (Murray *et al.*, 2007). In *L. japonicus* plants with a mutated *ckx3* gene encoding cytokinin oxidase, the number of infection threads was lower than that in wild-type plants; interestingly, treatment with the ethylene synthesis inhibitor aminoethoxyvinylglycine restored the number of infections. This observation indicates that cytokinins negatively affect the early stages of infection by ethylene signalling (Reid *et al.*, 2016). In our work, we demonstrated the absence of detectable amounts of *trans*-zeatin riboside in young infection threads in the nodules of the SGE wild type and in the 'locked' infection threads in *sym33-3* mutants. This cytokinin was also absent in young infection droplets in the wild-type nodules. However, in mature infection droplets, enhanced levels of *trans*-zeatin riboside were observed in wild-type nodules and in *sym33-3* and *sym26* mutant nodules. Surprisingly, *trans*-zeatin riboside was not detectable in hypertrophied infection droplets formed in nodules of the *sym40* mutant. The observed *trans*-zeatin riboside distribution may indicate that in mature nodules, some cytokinin forms are also involved in the negative regulation of infection, limiting infection thread growth and, specifically, the development of infection droplets. It should be noted that in the nodules of *sym33-2* and *sym33-3* mutants, the infection thread is highly ramified (Voroshilova *et al.*, 2009; Tsyganova *et al.*, 2019), probably because of decreased cytokinin levels and the absence of a negative cytokinin effect on infection thread growth.

Cytokinins promote bacteroid differentiation

It has been recently demonstrated in *A. hypogaea* with aeschynomenoid-type determinate nodules that gene silencing by *AhHK1-RNAi* dramatically inhibited the ability of bacteria to differentiate to bacteroids (Kundu and DasGupta, 2017). In this study, we used pea mutants accommodating different degrees of bacteroid differentiation. In the *sym31* mutants forming undifferentiated bacteroids (Borisov *et al.*, 1997), there was a significant decline in the signal intensity of the *trans*-zeatin riboside label associated with symbiosomes (Fig. 10D). However, in the *sym26* mutants forming nodules with morphologically differentiated bacteroids (Serova *et al.*, 2018), the signal intensity of the *trans*-zeatin riboside label associated with bacteroids resembled that in the SGE wild-type line (Fig. 10E). Hence, our results indicate a possible positive regulation of bacteroid differentiation by cytokinins in indeterminate nodules. Alternatively, the level of bacteroid differentiation may affect cytokinin accumulation in the infected cells of nodules. Thus, future experiments should examine the inter-relationships between both processes during nodulation.

Cytokinins negatively regulate nitrogen fixation in nodules

Another potential function of cytokinins in nodule formation could include controlling nitrogen fixation. It has been shown that cytokinin receptor inactivity results in reduced nodule formation and decreased nitrogen fixation in *M. truncatula cre1* mutants (Boivin *et al.*, 2016), whereas the use of kinetin in chickpea plants increased nitrogen fixation (Fatima *et al.*, 2008). However, the elevated cytokinin content in *L. japonicus ckx3-2* mutants, as well as in wild-type plants treated with the synthetic cytokinin 6-benzylaminopurine, enhanced the sensitivity of efficient nodule formation to nitrates, which demonstrates a negative effect of cytokinins on nitrogen fixation (Reid *et al.*, 2016). Our analysis detected a sharp reduction in the *trans*-zeatin riboside level in the nitrogen fixation zone of 4-week-old nodules during the active nitrogen fixation stage (Fig. 10A), which appears to correlate well with the negative effects of cytokinins on nitrogen fixation.

Thus, cytokinins may play a multifunctional role during the late stages of nodule development and the active nitrogen fixation stage. Our analysis using the *ipd3/cyclops* and *efd* pea mutants assessed the potential effect of cytokinins on plant cell and bacteroid differentiation, infection thread development, and nodule function.

SUPPLEMENTARY DATA

Supplementary data are available online at https://academic.oup.com/aob and consist of the following.

Figure S1: *trans*-zeatin riboside immunolocalization in control 2-week-old pea nodules.

Figure S2: visualization of auxin response maxima in the nodules of composite SGE pea wild-type plants containing the *DR5::GFP*-NLS construct.

Figure S3: N^6-isopentenyladenosine immunolocalization in the 2-week-old pea nodules of SGE wild type and *sym33-3* mutants.

Figure S4: *trans*-zeatin riboside immunolocalization in the 4-week-old pea nodules of SGE wild type and corresponding mutants.

Figure S5: *trans*-zeatin riboside immunolocalization in pea nodules of Sprint-2 wild type and *sym31* mutants.

Figure S6: expression pattern of cytokinin metabolic and regulatory genes in pea wild type and *sym33-2*, *sym33-3* and *sym40* mutants 3 weeks after inoculation.

Table S1: list of primers used in this study.

FUNDING

This work was financially supported by the Russian Science Foundation (grant 16-16-10043 for analysis of hormone

distribution in composite pea plants, grant 16-16-10035 for immunolocalization of cytokinins in root nodules).

ACKNOWLEDGEMENTS

We are very grateful to Dr Florian Frugier (IPS2, France) for providing the *pMtRR4::GUS* construct. The research was performed using equipment of the Core Centrum 'Genomic Technologies, Proteomics and Cell Biology' in ARRIAM, the Core Facilities Center 'Cell and Molecular Technologies in Plant Science' at the Komarov Botanical Institute RAS (Saint Petersburg, Russia) and Research Resource Centre 'Molecular and Cell Technologies' at the Saint Petersburg State University. The authors declare they have no competing interests.

LITERATURE CITED

Ariel F, Brault-Hernandez M, Laffont C, *et al.* 2012. Two direct targets of cytokinin signaling regulate symbiotic nodulation in *Medicago truncatula*. *The Plant Cell* **24**: 3838–3852.

Azarakhsh M, Kirienko AN, Zhukov VA, Lebedeva MA, Dolgikh EA, Lutova LA. 2015. KNOTTED1-LIKE HOMEOBOX 3: a new regulator of symbiotic nodule development. *Journal of Experimental Botany* **66**: 7181–7195.

Bielach A, Podlešáková K, Marhavý P, *et al.* 2012. Spatiotemporal regulation of lateral root organogenesis in *Arabidopsis* by cytokinin. *The Plant Cell* **24**: 3967–3981.

de Billy F, Grosjean C, May S, Bennett M, Cullimore JV. 2001. Expression studies on *AUX1*-like genes in *Medicago truncatula* suggest that auxin is required at two steps in early nodule development. *Molecular Plant-Microbe Interactions* **14**: 267–277.

Boivin S, Fonouni-Farde C, Frugier F. 2016. How auxin and cytokinin phytohormones modulate root microbe interactions. *Frontiers in Plant Science* **7**: 1240. doi: 10.3389/fpls.2016.01240.

Boot KJ, van Brussel AA, Tak T, Spaink HP, Kijne JW. 1999. Lipochitin oligosaccharides from *Rhizobium leguminosarum* bv. *viciae* reduce auxin transport capacity in *Vicia sativa* subsp. *nigra* roots. *Molecular Plant-Microbe Interactions* **12**: 839–844.

Borisov AY, Rozov S, Tsyganov V, *et al.* 1994. Identification of symbiotic genes in pea (*Pisum sativum* L.) by means of experimental mutagenesis. *Genetika (Russian Federation)* **30**: 1484–1494.

Borisov AY, Rozov SM, Tsyganov VE, Morzhina EV, Lebsky VK, Tikhonovich IA. 1997. Sequential functioning of *Sym-13* and *Sym-31*, two genes affecting symbiosome development in root nodules of pea (*Pisum sativum* L). *Molecular and General Genetics* **254**: 592–598.

Breakspear A, Liu C, Roy S, *et al.* 2014. The root hair 'infectome' of *Medicago truncatula* uncovers changes in cell cycle genes and reveals a requirement for auxin signaling in rhizobial infection. *The Plant Cell* **26**: 4680–4701.

Chen Y, Chen W, Li X, *et al.* 2014. Knockdown of *LjIPT3* influences nodule development in *Lotus japonicus*. *Plant & Cell Physiology* **55**: 183–193.

Cooper JB, Long SR. 1994. Morphogenetic rescue of *Rhizobium meliloti* nodulation mutants by trans-zeatin secretion. *The Plant Cell* **6**: 215–225.

Del Bianco M, Giustini L, Sabatini S. 2013. Spatiotemporal changes in the role of cytokinin during root development. *New Phytologist* **199**: 324–338.

Demina IV, Maity PJ, Nagchowdhury A, *et al.* 2019. Accumulation of and response to auxins in roots and nodules of the actinorhizal plant *Datisca glomerata* compared to the model legume *Medicago truncatula*. *Frontiers in Plant Science* **10**: 1085. doi: 10.3389/fpls.2019.01085

Denarie J, Debelle F, Prome J-C. 1996. Rhizobium lipo-chitooligosaccharide nodulation factors: signaling molecules mediating recognition and morphogenesis. *Annual Review of Biochemistry* **65**: 503–535.

Di Giacomo E, Laffont C, Sciarra F, Iannelli MA, Frugier F, Frugis G. 2017. KNAT3/4/5-like class 2 KNOX transcription factors are involved in *Medicago truncatula* symbiotic nodule organ development. *New Phytologist* **213**: 822–837.

Dolgikh EA, Shaposhnikov AI, Dolgikh AV, *et al.* 2017. Identification of *Pisum sativum* L. cytokinin and auxin metabolic and signaling genes, and an analysis of their role in symbiotic nodule development. *International Journal of Plant Physiology and Biochemistry* **9**: 22–35.

Dolgikh AV, Kirienko AN, Tikhonovich IA, Foo E, Dolgikh EA. 2019. The DELLA proteins influence the expression of cytokinin biosynthesis and response genes during nodulation. *Frontiers in Plant Science* **10**: 432. doi: 10.3389/fpls.2019.00432

Fåhraeus G. 1957. The infection of clover root hairs by nodule bacteria studied by a simple glass slide technique. *Journal of general microbiology* **16**: 374–381.

Fatima Z, Bano A, Sial R, Aslam M. 2008. Response of chickpea to plant growth regulators on nitrogen fixation and yield. *Pakistan Journal of Botany* **40**: 2005–2013.

Fisher J, Gaillard P, Fellbaum CR, Subramanian S, Smith S. 2018. Quantitative 3D imaging of cell level auxin and cytokinin response ratios in soybean roots and nodules. *Plant, Cell & Environment* **41**: 2080–2092.

Gamas P, Brault M, Jardinaud M-F, Frugier F. 2017. Cytokinins in symbiotic nodulation: when, where, what for? *Trends in Plant Science* **22**: 792–802.

Gonzalez-Rizzo S, Crespi M, Frugier F. 2006. The *Medicago truncatula* CRE1 cytokinin receptor regulates lateral root development and early symbiotic interaction with *Sinorhizobium meliloti*. *The Plant Cell* **18**: 2680–2693.

Hake S, Smith HMS, Holtan H, Magnani E, Mele G, Ramirez J. 2004. The role of *KNOX* genes in plant development. *Annual Review of Cell and Developmental Biology* **20**: 125–151.

Heckmann AB, Sandal N, Bek AS, *et al.* 2011. Cytokinin induction of root nodule primordia in *Lotus japonicus* is regulated by a mechanism operating in the root cortex. *Molecular Plant-Microbe Interactions* **24**: 1385–1395.

Held M, Hou H, Miri M, *et al.* 2014. *Lotus japonicus* cytokinin receptors work partially redundantly to mediate nodule formation. *The Plant Cell* **26**: 678–694.

Huo X, Schnabel E, Hughes K, Frugoli J. 2006. RNAi phenotypes and the localization of a protein::GUS fusion imply a role for *Medicago truncatula PIN* genes in nodulation. *Journal of Plant Growth Regulation* **25**: 156–165.

Ilina EL, Kiryushkin AS, Semenova VA, Demchenko NP, Pawlowski K, Demchenko KN. 2018. Lateral root initiation and formation within the parental root meristem of *Cucurbita pepo*: is auxin a key player? *Annals of Botany* **122**: 873–888.

Ioio RD, Linhares FS, Scacchi E, *et al.* 2007. Cytokinins determine *Arabidopsis* root-meristem size by controlling cell differentiation. *Current Biology* **17**: 678–682.

Ioio RD, Nakamura K, Moubayidin L, *et al.* 2008. A genetic framework for the control of cell division and differentiation in the root meristem. *Science* **322**: 1380–1384.

Ivanova KA, Tsyganova AV, Brewin NJ, Tikhonovich IA, Tsyganov VE. 2015. Induction of host defences by *Rhizobium* during ineffective nodulation of pea (*Pisum sativum* L.) carrying symbiotically defective mutations *sym40* (*PsEFD*), *sym33* (*PsIPD3/PsCYCLOPS*) and *sym42*. *Protoplasma* **252**: 1505–1517.

Ivanova MI, Todorov IT, Atanassova L, Dewitte W, Onckelen HAV. 1994. Co-localization of cytokinins with proteins related to cell proliferation in developing somatic embryos of *Dactylis glomerata* L. *Journal of Experimental Botany* **45**: 1009–1017.

Jardinaud M-F, Boivin S, Rodde N, *et al.* 2016. A laser dissection-RNAseq analysis highlights the activation of cytokinin pathways by Nod factors in the *Medicago truncatula* root epidermis. *Plant Physiology* **171**: 2256–2276.

Jin D, Meng X, Wang Y, Wang J, Zhao Y, Chen M. 2020. Expression and regulation of small RNAs in the plant–microorganism symbioses in *Medicago truncatula*. In: de Bruijn FJ, ed. *The model legume Medicago truncatula*. Hoboken: John Wiley and Sons, 919–922.

Kärkönen A, Simola LK. 1999. Localization of cytokinins in somatic and zygotic embryos of *Tilia cordata* using immunocytochemistry. *Physiologia Plantarum* **105**: 355–365.

Kisiala A, Laffont C, Emery RJN, Frugier F. 2013. Bioactive cytokinins are selectively secreted by *Sinorhizobium meliloti* nodulating and nonnodulating strains. *Molecular Plant-Microbe Interactions* **26**: 1225–1231.

Kitaeva AB, Demchenko KN, Tikhonovich IA, Timmers ACJ, Tsyganov VE. 2016. Comparative analysis of the tubulin cytoskeleton organization in nodules of *Medicago truncatula* and *Pisum sativum*: bacterial release and

bacteroid positioning correlate with characteristic microtubule rearrangements. *New Phytologist* **210**: 168–183.

Kosterin OE, Rozov SM. 1993. Mapping of the new mutation *blb* and the problem of integrity of linkage group I. *Pisum Genetics* **25**: 27–31.

Kundu A, DasGupta M. 2017. Silencing of putative cytokinin receptor histidine kinase1 inhibits both inception and differentiation of root nodules in *Arachis hypogae*. *Molecular Plant-Microbe Interactions* **31**: 187–199.

Laplaze L, Benkova E, Casimiro I, *et al.* 2007. Cytokinins act directly on lateral root founder cells to inhibit root initiation. *The Plant Cell* **19**: 3889–3900.

Laplaze L, Lucas M, Champion A. 2015. Rhizobial root hair infection requires auxin signaling. *Trends in Plant Science* **20**: 332–334.

Leppyanen IV, Kirienko AN, Dolgikh EA. 2019. *Agrobacterium rhizogenes*-mediated transformation of *Pisum sativum* L. roots as a tool for studying the mycorrhizal and root nodule symbioses. *PeerJ* **7**: e6552. doi: 10.7717/peerj.6552

Libbenga KR, Harkes PAA. 1973. Initial proliferation of cortical cells in the formation of root nodules in *Pisum sativum* L. *Planta* **114**: 17–28.

Liu J, Rutten L, Limpens E, *et al.* 2018. A remote *cis*-regulatory region is required for *NIN* expression in the pericycle to initiate nodule primordium formation in *Medicago truncatula*. *The Plant Cell* **31**: 68–83.

Livak KJ, Schmittgen TD. 2001. Analysis of relative gene expression data using real-time quantitative PCR and the $2^{-\Delta\Delta Ct}$ method. *Methods* **25**: 402–408.

Lohar DP, Schaff JE, Laskey JG, Kieber JJ, Bilyeu KD, Bird DM. 2004. Cytokinins play opposite roles in lateral root formation, and nematode and rhizobial symbioses. *The Plant Journal* **38**: 203–214.

Lohar DP, Sharopova N, Endre G, *et al.* 2006. Transcript analysis of early nodulation events in *Medicago truncatula*. *Plant Physiology* **140**: 221–234.

Mathesius U, Schlaman HRM, Spaink HP, Of Sautter C, Rolfe BG, Djordjevic MA. 1998. Auxin transport inhibition precedes root nodule formation in white clover roots and is regulated by flavonoids and derivatives of chitin oligosaccharides. *The Plant Journal* **14**: 23–34.

Messinese E, Mun J-H, Yeun LH, *et al.* 2007. A novel nuclear protein interacts with the symbiotic DMI3 calcium- and calmodulin-dependent protein kinase of *Medicago truncatula*. *Molecular Plant-Microbe Interactions* **20**: 912–921.

Mortier V, Wasson A, Jaworek P, *et al.* 2014. Role of *LONELY GUY* genes in indeterminate nodulation on *Medicago truncatula*. *New Phytologist* **202**: 582–593.

Moubayidin L, Perilli S, Ioio RD, Di Mambro R, Costantino P, Sabatini S. 2010. The rate of cell differentiation controls the *Arabidopsis* root meristem growth phase. *Current Biology* **20**: 1138–1143.

Murray JD, Karas BJ, Sato S, Tabata S, Amyot L, Szczyglowski K. 2007. A cytokinin perception mutant colonized by *Rhizobium* in the absence of nodule organogenesis. *Science* **315**: 101–104.

Nemankin N. 2011. *Analysis of pea (Pisum sativum L.) genetic system, controlling development of arbuscular mycorrhiza and nitrogen-fixing symbiosis*. PhD thesis (in Russian), Saint-Petersburg State University, Russia.

Ng JLP, Hassan S, Truong TT, *et al.* 2015. Flavonoids and auxin transport inhibitors rescue symbiotic nodulation in the *Medicago truncatula* cytokinin perception mutant *cre1*. *The Plant Cell* **27**: 2210–2226.

Op den Camp RHM, De Mita S, Lillo A, *et al.* 2011. A phylogenetic strategy based on a legume-specific whole genome duplication yields symbiotic cytokinin type-A response regulators. *Plant Physiology* **157**: 2013–2022.

Ovchinnikova E, Journet E-P, Chabaud M, *et al.* 2011. IPD3 controls the formation of nitrogen-fixing symbiosomes in pea and *Medicago* spp. *Molecular Plant-Microbe Interactions* **24**: 1333–1344.

Pacios-Bras C, Schlaman HRM, Boot K, *et al.* 2003. Auxin distribution in *Lotus japonicus* during root nodule development. *Plant Molecular Biology* **52**: 1169–1180.

Plet J, Wasson A, Ariel F, *et al.* 2011. MtCRE1-dependent cytokinin signaling integrates bacterial and plant cues to coordinate symbiotic nodule organogenesis in *Medicago truncatula*. *The Plant Journal* **65**: 622–633.

Quandt HJ, Pühler A, Broer I. 1993. Transgenic root nodules of *Vicia hirsuta*: a fast and efficient system for the study of gene expression in indeterminate-type nodules. *Molecular Plant-Microbe Interactions* **6**: 699–706.

Reid DE, Heckmann AB, Novák O, Kelly S, Stougaard J. 2016. CYTOKININ OXIDASE/DEHYDROGENASE3 maintains cytokinin homeostasis during root and nodule development in *Lotus japonicus*. *Plant Physiology* **170**: 1060–1074.

Reid DE, Nadzieja M, Novak O, Heckmann AB, Sandal N, Stougaard J. 2017. Cytokinin biosynthesis promotes cortical cell responses during nodule development. *Plant Physiology* **175**: 361–375.

Ren B, Wang X, Duan J, Ma J. 2019. Rhizobial tRNA-derived small RNAs are signal molecules regulating plant nodulation. *Science* **365**: 919–922.

Rightmyer AP, Long SR. 2011. Pseudonodule formation by wild-type and symbiotic mutant *Medicago truncatula* in response to auxin transport inhibitors. *Molecular Plant-Microbe Interactions* **24**: 1372–1384.

Roy S, Robson FC, Lilley JLS, *et al.* 2017. MtLAX2, a functional homologue of the auxin importer AtAUX1, is required for nodule organogenesis. *Plant Physiology* **174**: 326–338.

Schiessl K, Lilley JLS, Lee T, *et al.* 2019. *NODULE INCEPTION* recruits the lateral root developmental program for symbiotic nodule organogenesis in *Medicago truncatula*. *Current Biology* **29**: 3657–3668.

Serova TA, Tsyganova AV, Tsyganov VE. 2018. Early nodule senescence is activated in symbiotic mutants of pea (*Pisum sativum* L.) forming ineffective nodules blocked at different nodule developmental stages. *Protoplasma* **255**: 1443–1459.

Simon SA, Meyers BC, Sherrier DJ. 2009. MicroRNAs in the rhizobia legume symbiosis. *Plant Physiology* **151**: 1002–1008.

Singh S, Katzer K, Lambert J, Cerri M, Parniske M. 2014. CYCLOPS, a DNA-binding transcriptional activator, orchestrates symbiotic root nodule development. *Cell Host and Microbe* **15**: 139–152.

Suzaki T, Yano K, Ito M, Umehara Y, Suganuma N, Kawaguchi M. 2012. Positive and negative regulation of cortical cell division during root nodule development in *Lotus japonicus* is accompanied by auxin response. *Development* **139**: 3997–4006.

Suzaki T, Ito M, Yoro E, *et al.* 2014. Endoreduplication-mediated initiation of symbiotic organ development in *Lotus japonicus*. *Development* **141**: 2441–2445.

Syōno K, Newcomb W, Torrey JG. 1976. Cytokinin production in relation to the development of pea root nodules. *Canadian Journal of Botany* **54**: 2155–2162.

Takahashi N, Kajihara T, Okamura C, *et al.* 2013. Cytokinins control endocycle onset by promoting the expression of an APC/C activator in *Arabidopsis* roots. *Current Biology* **23**: 1812–1817.

Thimann KV. 1936. On the physiology of the formation of nodules on legume roots. *Proceedings of the National Academy of Sciences, USA* **22**: 511–514.

Tirichine L, Sandal N, Madsen LH, *et al.* 2007. A gain-of-function mutation in a cytokinin receptor triggers spontaneous root nodule organogenesis. *Science* **315**: 104–107.

Tsyganov VE, Borisov AY, Rozov SM, Tikhonovich IA. 1994. New symbiotic mutants of pea obtained after mutagenesis of laboratory line SGE. *Pisum Genetics* **26**: 36–37.

Tsyganov VE, Morzhina EV, Stefanov SY, Borisov AY, Lebsky VK, Tikhonovich IA. 1998. The pea (*Pisum sativum* L.) genes *sym33* and *sym40* control infection thread formation and root nodule function. *Molecular and General Genetics* **259**: 491–503.

Tsyganov VE, Voroshilova VA, Borisov AY, Tikhonovich IA, Rozov SM. 2000. Four more symbiotic mutants obtained using EMS mutagenesis of line SGE. *Pisum Genetics* **32**: 63.

Tsyganov VE, Seliverstova E, Voroshilova V, *et al.* 2011. Double mutant analysis of sequential functioning of pea (*Pisum sativum* L.) genes *Sym13*, *Sym33*, and *Sym40* during symbiotic nodule development. *Russian Journal of Genetics: Applied Research* **1**: 343.

Tsyganov VE, Voroshilova V, Rozov S, Borisov AY, Tikhonovich I. 2013. A new series of pea symbiotic mutants induced in the line SGE. *Russian Journal of Genetics: Applied Research* **3**: 156–162.

Tsyganova AV, Tsyganov VE, Findlay KC, Borisov AY, Tikhonovich IA, Brewin NG. 2009. Distribution of legume arabinogalactanprotein-extensin (AGPE) glycoproteins in symbiotically defective pea mutants with abnormal infection threads. *Cell and Tissue Biology* **51**: 93–102.

Tsyganova AV, Ivanova KA, Tsyganov VE. 2019. Histological and ultrastructural nodule organization of the pea (*Pisum sativum*) mutant SGEFix–5 in the *Sym33* gene encoding the transcription factor PsCYCLOPS/PsIPD3. *Ecological genetics* **17**: 65–70.

Vernié T, Moreau S, de Billy F, *et al.* 2008. EFD is an ERF transcription factor involved in the control of nodule number and differentiation in *Medicago truncatula*. *The Plant Cell* **20**: 2696–2713.

Vernié T, Kim J, Frances L, *et al.* 2015. The NIN transcription factor coordinates diverse nodulation programs in different tissues of the *Medicago truncatula* root. *The Plant Cell* **27**: 3410–3424.

Voroshilova VA, Boesten B, Tsyganov VE, Borisov AY, Tikhonovich IA, Priefer UB. 2001. Effect of mutations in *Pisum sativum* L. genes blocking

different stages of nodule development on the expression of late symbiotic genes in *Rhizobium leguminosarum* bv. *viciae*. *Molecular Plant-Microbe Interactions* **14**: 471–476.

Voroshilova VA, Demchenko KN, Brewin NJ, Borisov AY, Tikhonovich IA. 2009. Initiation of a legume nodule with an indeterminate meristem involves proliferating host cells that harbour infection threads. *New Phytologist* **181**: 913–923.

Wang TL, Wood EA, Brewin NJ. 1982. Growth regulators, *Rhizobium* and nodulation in peas. *Planta* **155**: 350–355.

Yano K, Yoshida S, Müller J, *et al.* 2008. CYCLOPS, a mediator of symbiotic intracellular accommodation. *Proceedings of the National Academy of Sciences, USA* **105**: 20540–20545.

Yoon HJ, Hossain MS, Held M, *et al.* 2014. *Lotus japonicus SUNERGOS1* encodes a predicted subunit A of a DNA topoisomerase VI that is required for nodule differentiation and accommodation of rhizobial infection. *The Plant Journal* **78**: 811–821.

van Zeijl A, den Camp RHO, Deinum EE, *et al.* 2015. *Rhizobium* lipo-chitooligosaccharide signaling triggers accumulation of cytokinins in *Medicago truncatula* roots. *Molecular Plant* **8**: 1213–1226.

Zhernakov AI, Shtark OY, Kulaeva OA, *et al.* 2019. Mapping-by-sequencing using NGS-based 3′-MACE-Seq reveals a new mutant allele of the essential nodulation gene *Sym33* (*IPD3*) in pea (*Pisum sativum* L.). *PeerJ* **7**: e6662. doi: 10.7717/peerj.6662